1

Thermodynamics and Phase Diagrams

This chapter deals with some of the basic thermodynamic concepts that are required for a more fundamental appreciation of phase diagrams and phase transformations. It is assumed that the reader is already acquainted with elementary thermodynamics and only a summary of the most important results as regards phase transformations will be given here. Fuller treatment can be found in the books listed at the end of this chapter.

The main use of thermodynamics in physical metallurgy is to allow the predication of whether an alloy is in equilibrium. In considering phase transformations we are always concerned with changes toward equilibrium, and thermodynamics is therefore a very powerful tool. It should be noted, however, that rate at which equilibrium is reached cannot be determined by thermodynamics alone, as will become apparent in later chapters.

1.1 Equilibrium

It is useful to begin this chapter on thermodynamics by defining a few of the terms that will be frequently used. In the study of phase transformations, we will be dealing with the changes that can occur within a given system, e.g., an alloy that can exist as a mixture of one or more phases. A phase can be defined as a portion of the system whose properties and composition are homogeneous and which is physically distinct from other parts of the system. The components of a given system are the different elements or chemical compounds which make up the system, and the composition of a phase or the system can be described by giving the relative amounts of each component.

The study of phase transformations, as the name suggests, is concerned with how one or more phases in an alloy (the system) change into a new phase or mixture of phases. The reason why a transformation occurs at all is because the initial state of the alloy is unstable relative to the final state. But how is phase stability measured? The answer to this question is provided by thermodynamics. For transformations that occur at constant temperature and pressure, the relative stability of a system is determined by its Gibbs free energy (G).

The Gibbs free energy of a system is defined by the equation

$$G = H - TS \tag{1.1}$$

where
H is the enthalpy
T is the absolute temperature
S is the entropy of the system

Enthalpy is a measure of the heat content of the system and is given by

$$H = E + PV \tag{1.2}$$

where
E is the internal energy of the system
P is the pressure
V is the volume

The internal energy arises from the total kinetic and potential energies of the atoms within the system. Kinetic energy can arise from atomic vibration in solids or liquids and from translational and rotational energies for the atoms and molecules within a liquid or gas; whereas potential energy arises from the interactions, or bonds, between the atoms within the system. If a transformation or reaction occurs the heat that is absorbed or evolved will depend on the change in the internal energy of the system. However, it will also depend on changes in the volume of the system and the term PV takes this into account, so that at constant pressure the heat absorbed or evolved is given by the change in H. When dealing with condensed phases (solids and liquids) the PV term is usually very small in comparison to E, that is, $H \approx E$. This approximation will be made frequently in the treatments given in this book. The other function that appears in the expression for G is entropy (S) which is a measure of the randomness of the system.

A system is said to be in equilibrium when it is in the most stable state, i.e., shows no desire to change ad infinitum. An important consequence of the laws of classical thermodynamics is that at constant temperature and pressure a closed system (i.e., one of fixed mass and composition) will be in stable equilibrium if it has the lowest possible value of the Gibbs free energy, or in mathematical terms

$$dG = 0 \tag{1.3}$$

It can be seen from the definition of G (Equation 1.1) that the state with the highest stability will be that with the best compromise between low enthalpy and high entropy. Thus at low temperatures, solid phases are most stable since they have the strongest atomic binding and therefore the lowest internal energy (enthalpy). At high temperatures, however, the $-TS$ term

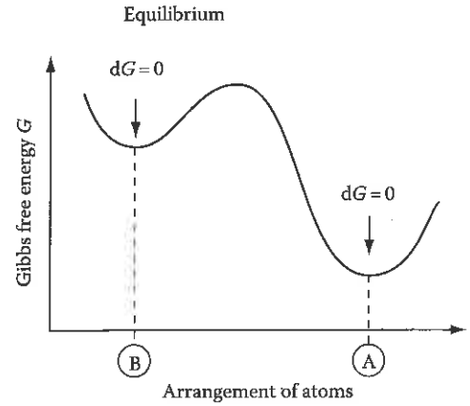

FIGURE 1.1
Schematic variation of Gibbs free energy with the arrangement of atoms. Configuration "A" has the lowest free energy and is therefore the arrangement when the system is at stable equilibrium. Configuration "B" is a metastable equilibrium.

dominates and phases with more freedom of atom movement, liquids and gases, become most stable. If pressure changes are considered it can be seen from Equation 1.2 that phases with small volumes are favored by high pressures.

The definition of equilibrium given by Equation 1.3 can be illustrated graphically as follows. If it were possible to evaluate the free energy of a given system for all conceivable configurations the stable equilibrium configuration would be found to have the lowest free energy. This is illustrated in Figure 1.1 where it is imagined that the various atomic configurations can be represented by points along the abscissa. Configuration A would be the stable equilibrium state. At this point small changes in the arrangement of atoms to a first approximation produce no change in G, i.e., Equation 1.3 applies. However, there will always be other configurations, e.g., B, which lie at a local minimum in free energy and therefore also satisfy Equation 1.3, but which do not have the lowest possible value of G. Such configurations are called metastable equilibrium states to distinguish them from the stable equilibrium state. The intermediate states for which $dG \neq 0$ are unstable and are only ever realized momentarily in practice. If, as result of thermal fluctuations, the atoms become arranged in an intermediate state they will rapidly rearrange into one of the free energy minima. If by a change of temperature or pressure, for example, a system is moved from a stable to a metastable state it will, given time, transform to the new stable equilibrium state.

Graphite and diamond at room temperature and pressure are examples of stable and metastable equilibrium states. Given time, therefore, all diamond under these conditions will transform to graphite.

Any transformation that results in a decrease in Gibbs free energy is possible. Therefore, a necessary criterion for any phase transformation is

$$\Delta G = G_2 - G_1 < 0 \tag{1.4}$$

where G_1 and G_2 are the free energies of the initial and final states, respectively. The transformation need not go directly to the stable equilibrium state but can pass through a whole series of intermediate metastable states.

The answer to the question "How fast does a phase transformation occur?" is not provided by classical thermodynamics. Sometimes metastable states can be very short-lived; at other times they can exist almost indefinitely as in the case of diamond at room temperature and pressure. The reason for these differences is the presence of the free energy hump between the metastable and stable states in Figure 1.1. The study of transformation rates in physical chemistry belongs to the realm of kinetics. In general, higher humps or energy barriers lead to slower transformation rates. Kinetics obviously plays a central role in the study of phase transformations and many examples of kinetic processes will be found throughout this book.

The different thermodynamic functions that have been mentioned in this section can be divided into two types called intensive and extensive properties. The intensive properties are those which are independent of the size of the system such as T and P, whereas the extensive properties are directly proportional to the quantity of material in the system, e.g., V, E, H, S, and G. The usual way of measuring the size of the system is by the number of moles of material it contains. The extensive properties are then molar quantities, i.e., expressed in units per mole. The number of moles of a given component in the system is given by the mass of the component in grams divided by its atomic or molecular weight.

The number of atoms or molecules within 1 mol of material is given by Avogadro's number (N_a) and is 6.023×10^{23}.

1.2 Single-Component Systems

Let us begin by dealing with the phase changes that can be induced in a single component by changes in temperature at a fixed pressure, say 1 atm. A single-component system could be one containing a pure element or one type of molecule that does not dissociate over the range of temperature of interest. In order to predict the phases that are stable or mixtures that are in equilibrium at different temperatures it is necessary to be able to calculate the variation of G with T.

1.2.1 Gibbs Free Energy as a Function of Temperature

The specific heat of most substances is easily measured and readily available. In general, it varies with temperature as shown in Figure 1.2a. The specific heat is the quantity of heat (in J) required to raise the temperature of the substance by 1 K. At constant pressure this is denoted by C_p and is given by

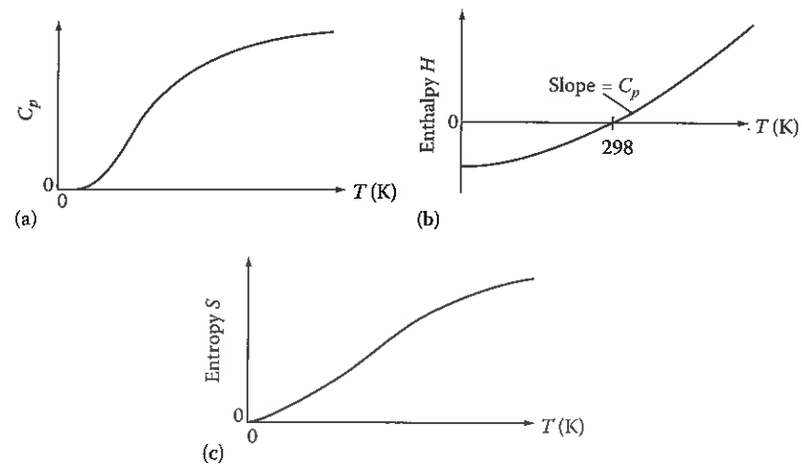

FIGURE 1.2
(a) Variation of C_p with temperature, C_p tends to a limit of ~3R. (b)Variation of enthalpy (H) with absolute temperature for a pure metal. (c) Variation of entropy (S) with absolute temperature.

$$C_p = \left(\frac{\partial H}{\partial T}\right)_p \tag{1.5}$$

Therefore, the variation of H with T can be obtained from a knowledge of the variation of C_p with T. In considering phase transformations or chemical reactions it is only changes in thermodynamic functions that are of interest. Consequently, H can be measured relative to any reference level which is usually done by defining $H = 0$ for a pure element in its most stable state at 298 K (25°C). The variation of H with T can then be calculated by integrating Equation 1.5, i.e.,

$$H = \int_{298}^{T} C_p \, dT \tag{1.6}$$

The variation is shown schematically in Figure 1.2b. The slope of the H–T curve is C_p.

The variation of entropy with temperature can also be derived from the specific heat C_p. From classical thermodynamics

$$\frac{C_p}{T} = \left(\frac{\partial S}{\partial T}\right)_p \tag{1.7}$$

Taking entropy at 0 K as zero, Equation 1.7 can be integrated to give

$$S = \int_{0}^{T} \frac{C_p}{T} dT \tag{1.8}$$

as shown in Figure 1.2c.

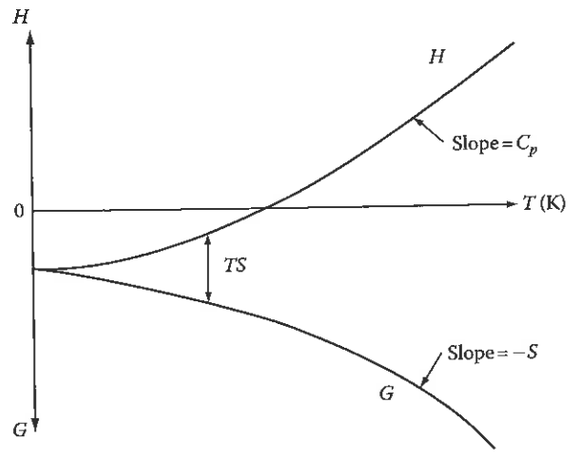

FIGURE 1.3
Variation of Gibbs free energy with temperature.

Finally the variation of G with temperature shown in Figure 1.3 is obtained by combining Figure 1.2b and c using Equation 1.1. When temperature and pressure vary the change in Gibbs free energy can be obtained from the following result of classical thermodynamics: for a system of fixed mass and composition:

$$dG = -S\,dT + V\,dP \tag{1.9}$$

At constant pressure $dP = 0$ and

$$\left(\frac{\partial G}{\partial T}\right)_p = -S \tag{1.10}$$

This means that G decreases with increasing T at a rate given by $-S$. The relative positions of the free energy curves of solid and liquid phases are illustrated in Figure 1.4. At all temperatures the liquid has a higher enthalpy (internal energy) than the solid. Therefore, at low temperatures $G^L > G^S$. However, the liquid phase has a higher entropy than the solid phase and the Gibbs free energy of the liquid therefore decreases more rapidly with increasing temperature than that of the solid. For temperatures up to T_m the solid phase has the lowest free energy and is therefore the stable equilibrium phase, whereas above T_m the liquid phase is the equilibrium state of the system. At T_m both phases have the same value of G and both solid and liquid can exist in equilibrium. T_m is therefore the equilibrium melting temperature at the pressure concerned.

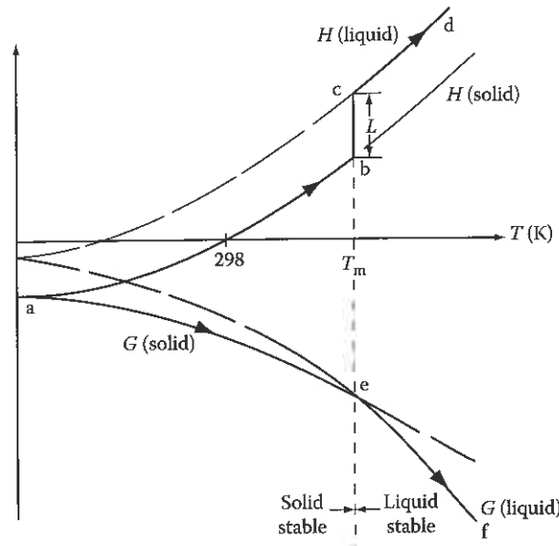

FIGURE 1.4
Variation of enthalpy (H) and free energy (G) with temperature for the solid and liquid phases of a pure metal. L is the latent heat of melting. T_m is the equilibrium melting temperature.

If a pure component is heated from absolute zero the heat supplied will raise the enthalpy at a rate determined by C_p (solid) along the line ab in Figure 1.4. Meanwhile the free energy will decrease along ae. At T_m the heat supplied to the system will not raise its temperature but will be used in supplying the latent heat of melting (L) that is required to convert solid into liquid (bc in Figure 1.4). Note that at T_m the specific heat appears to be infinite since the addition of heat does not appear as an increase in temperature. When all solid has transformed into liquid the enthalpy of the system will follow the line cd while the Gibbs free energy decreases along ef. At still higher temperatures than shown in Figure 1.4 the free energy of the gas phase (at atmospheric pressure) becomes lower than that of the liquid and the liquid transforms to a gas. If the solid phase can exist in different crystal structures (allotropes or polymorphs) free energy curves can be constructed for each of these phases and the temperature at which they intersect will give the equilibrium temperature for the polymorphic transformation. For example, at atmospheric pressure iron can exist as either body-centered cubic (bcc) ferrite below 910°C or face-centered cubic (fcc) austenite above 910°C, and at 910°C both phases can exist in equilibrium.

1.2.2 Pressure Effects

The equilibrium temperatures discussed so far only apply at a specific pressure (1 atm, say). At other pressures the equilibrium temperatures will differ. For example, Figure 1.5 shows the effect of pressure on the equilibrium temperatures for pure iron. Increasing pressure has the effect of depressing the α/γ equilibrium temperature and raising the equilibrium melting

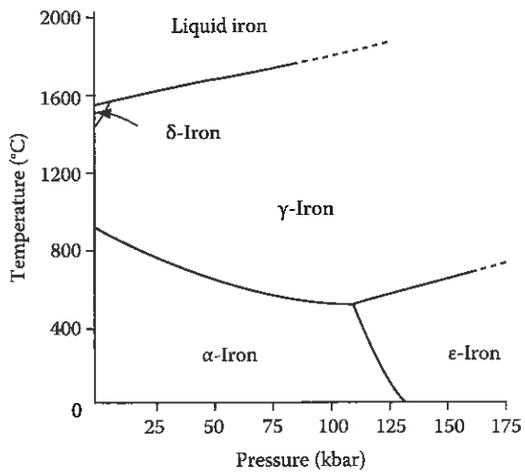

FIGURE 1.5
Effect of pressure on the equilibrium phase diagram for pure iron.

temperature. At very high pressures hexagonal close-packed (hcp) ε-Fe becomes stable. The reason for these changes derives from Equation 1.9. At constant temperature the free energy of a phase increases with pressure such that

$$\left(\frac{\partial G}{\partial P}\right)_T = V \tag{1.11}$$

If the two phases in equilibrium have different molar volumes their respective free energies will not increase by the same amount at a given temperature and equilibrium will, therefore, be disturbed by changes in pressure. The only way to maintain equilibrium at different pressure is by varying the temperature.

If the two phases in equilibrium are α and β, application of Equation 1.9 to 1 mol of both gives

$$\begin{aligned} dG^\alpha &= V_m^\alpha\, dP - S^\alpha\, dT \\ dG^\beta &= V_m^\beta\, dP - S^\beta\, dT \end{aligned} \tag{1.12}$$

If α and β are in equilibrium $G^\alpha = G^\beta$ therefore $dG^\alpha = dG^\beta$ and

$$\left(\frac{dP}{dT}\right)_{eq} = \frac{S^\beta - S^\alpha}{V_m^\beta - V_m^\alpha} = \frac{\Delta S}{\Delta V} \tag{1.13}$$

This equation gives the change in temperature of dT required to maintain equilibrium between α and β if pressure is increased by dP. The equation can be simplified as follows. From Equation 1.1

$$\begin{aligned} G^\alpha &= H^\alpha - TS^\alpha \\ G^\beta &= H^\beta - TS^\beta \end{aligned}$$

Therefore, putting $\Delta G = G^\beta - G^\alpha$, etc., gives

$$\Delta G = \Delta H - T\Delta S$$

But since at equilibrium $G^\beta - G^\alpha$, $\Delta G = 0$, and

$$\Delta H - T\Delta S = 0$$

Consequently, Equation 1.13 becomes

$$\left(\frac{dP}{dT_{eq}}\right) = \frac{\Delta H}{T_{eq}\Delta V} \tag{1.14}$$

which is known as the Clausius–Clapeyron equation. Since close-packed γ-Fe has a smaller molar volume than α-Fe, $\Delta V = V_m^\gamma - V_m^\alpha < 0$ whereas $\Delta H = H^\gamma - H^\alpha > 0$ (for the same reason that a liquid has a higher enthalpy than a solid), so that (dP/dT) is negative, i.e., an increase in pressure lowers the equilibrium transition temperature. On the other hand the δ/L equilibrium temperature is raised with increasing pressure due to the larger molar volume of the liquid phase. It can be seen that the effect of increasing pressure is to increase the area of the phase diagram over which the phase with the smallest molar volume is stable (γ-Fe in Figure 1.5). It should also be noted that ε-Fe has the highest density of the three allotropes, consistent with the slopes of the phase boundaries in the Fe phase diagram.

1.2.3 Driving Force for Solidification

In dealing with phase transformations, we are often concerned with the difference in free energy between two phases at temperatures away from the equilibrium temperature. For example, if a liquid metal is undercooled by ΔT below T_m before it solidifies, solidification will be accompanied by a decrease in free energy ΔG (J mol^{-1}) as shown in Figure 1.6. This free energy decrease provides the driving force for solidification. The magnitude of this change can be obtained as follows.

The free energies of the liquid and solid at a temperature T are given by

$$\begin{aligned} G^L &= H^L - TS^L \\ G^S &= H^S - TS^S \end{aligned}$$

Therefore, at a temperature T

$$\Delta G = \Delta H - T\Delta S \tag{1.15}$$

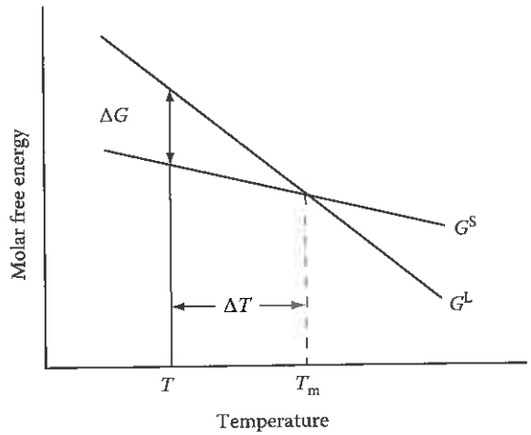

FIGURE 1.6
Difference in free energy between liquid and solid close to the melting point. The curvature of the G^S and G^L lines has been ignored.

where

$$\Delta H = H^L - H^S \quad \text{and} \quad \Delta S = S^L - S^S$$

At the equilibrium melting temperature T_m the free energies of solid and liquid are equal, i.e., $\Delta G = 0$. Consequently

$$\Delta G = \Delta H - T_m \Delta S = 0$$

and therefore at T_m

$$\Delta S = \frac{\Delta H}{T_m} = \frac{L}{T_m} \tag{1.16}$$

This is known as the entropy of fusion. It is observed experimentally that the entropy of fusion is a constant $\simeq R$ (8.3 J mol^{-1} K^{-1}) for most metals (Richard's rule). This is not unreasonable as metals with high bond strengths can be expected to have high values for both L and T_m.

For small undercoolings (ΔT) the difference in the specific heats of the liquid and solid ($C_p^L - C_p^S$) can be ignored. ΔH and ΔS are therefore approximately independent of temperature. Combining Equations 1.15 and 1.16 thus gives

$$\Delta G \simeq L - T\frac{L}{T_m}$$

i.e., for small ΔT

$$\Delta G \simeq \frac{L\Delta T}{T_m} \tag{1.17}$$

This is a very useful result which will frequently recur in subsequent chapters.

1.3 Binary Solutions

In single-component systems all phases have the same composition, and equilibrium simply involves pressure and temperature as variables. In alloys, however, composition is also variable and to understand phase changes in alloys requires an appreciation of how the Gibbs free energy of a given phase depends on composition as well as temperature and pressure. Since the phase transformations described in this book mainly occur at a fixed pressure of 1 atm most attention will be given to changes in composition and temperature. In order to introduce some of the basic concepts of the thermodynamics of alloys a simple physical model for binary solid solutions will be described.

1.3.1 Gibbs Free Energy of Binary Solutions

The Gibbs free energy of a binary solution of A and B atoms can be calculated from the free energies of pure A and B in the following way.

It is assumed that A and B have the same crystal structures in their pure states and can be mixed in any proportions to make a solid solution with the same crystal structure. Imagine that 1 mol of homogeneous solid solution is made by mixing together X_A mol of A and X_B mol of B. Since there is a total of 1 mol of solution

$$X_A + X_B = 1 \tag{1.18}$$

where X_A and X_B are the mole fractions of A and B, respectively, in the alloy. In order to calculate the free energy of the alloy, the mixing can be made in two steps (Figure 1.7). They are

1. Bring together X_A mol of pure A and X_B mol of pure B
2. Allow the A and B atoms to mix together to make a homogeneous solid solution

After step 1 the free energy of the system is given by

$$G_1 = X_A G_A + X_B G_B \text{ (J mol}^{-1}\text{)} \tag{1.19}$$

where G_A and G_B are the molar free energies of pure A and B at the temperature and pressure of the above experiment. G_1 can be most

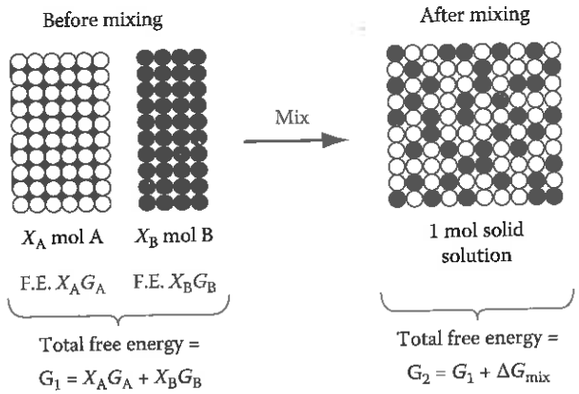

FIGURE 1.7
Free energy of mixing.

conveniently represented on a molar free energy diagram (Figure 1.8) in which molar free energy is plotted as a function of X_B or X_A. For all alloy compositions G_1 lies on the straight line between G_A and G_B.

The free energy of the system will not remain constant during the mixing of the A and B atoms and after step 2 the free energy of the solid solution G_2 can be expressed as

$$G_2 = G_1 + \Delta G_{mix} \tag{1.20}$$

where ΔG_{mix} is the change in Gibbs free energy caused by the mixing.

Since

$$G_1 = H_1 - TS_1$$

and

$$G_2 = H_2 - TS_2$$

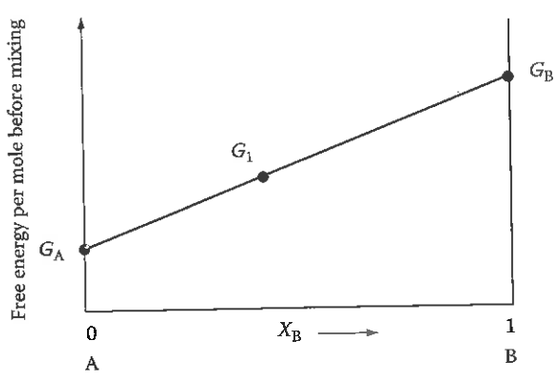

FIGURE 1.8
Variation of G_1 (the free energy before mixing) with alloy composition (X_A or X_B).

putting

$$\Delta H_{mix} = H_2 - H_1$$

and

$$\Delta S_{mix} = S_2 - S_1$$

gives

$$\Delta G_{mix} = \Delta H_{mix} - T\Delta S_{mix} \tag{1.21}$$

where ΔH_{mix} is the heat absorbed or evolved during step 2, i.e., it is the heat of solution, and ignoring volume changes during the process, it represents only the difference in internal energy (E) before and after mixing. ΔS_{mix} is the difference in entropy between the mixed and unmixed states.

1.3.2 Ideal Solutions

The simplest type of mixing to treat first is when $\Delta H_{mix} = 0$, in which case the resultant solution is said to be ideal and the free energy change on mixing is only due to the change in entropy

$$\Delta G_{mix} = -T\Delta S_{mix} \tag{1.22}$$

In statistical thermodynamics, entropy is quantitatively related to randomness by the Boltzmann equation, i.e.,

$$S = k \ln \omega \tag{1.23}$$

where
k is Boltzmann's constant
ω is a measure of randomness

There are two contributions to the entropy of a solid solution—a thermal contribution S_{th} and configurational contribution S_{config}.

In the case of thermal entropy, ω is the number of ways in which the thermal energy of the solid can be divided among the atoms, that is, the total number of ways in which vibrations can be set up in the solid. In solutions, additional randomness exists due to the different ways in which the atoms can be arranged. This gives extra entropy S_{config} for which ω is the number of distinguishable ways of arranging the atoms in the solution.

If there is no volume change or heat change or heat change during mixing then the only contribution to ΔS_{mix} is the change in configurational entropy. Before mixing, the A and B atoms are held separately in the system and there is only one distinguishable way in which the atoms can be arranged. Consequently $S_1 = k \ln 1 = 0$ and therefore $\Delta S_{mix} = S_2$.

Assuming that A and B mix to form a substitutional solid solution and that all configurations of A and B atoms are equally probable, the number of distinguishable ways of arranging the atoms on the atom site is

$$\omega_{\text{config}} = \frac{(N_A + N_B)!}{N_A! N_B!} \tag{1.24}$$

where
N_A is the number of A atoms
N_B is the number of B atoms

Since we are dealing with 1 mol of solution, i.e., N_a atoms (Avogadro's number),

$$N_A = X_A N_a$$

and

$$N_B = X_B N_a$$

By substituting into Equations 1.23 and 1.24, using Stirling's approximation ($\ln N! \simeq N \ln N - N$) and the relationship $N_a k = R$ (the universal gas constant) gives

$$\Delta S_{\text{mix}} = -R(X_A \ln X_A + X_B \ln X_B) \tag{1.25}$$

Note that, since X_A and X_B are less than unity, ΔS_{mix} is positive, i.e., there is an increase in entropy on mixing, as expected. The free energy of mixing, ΔG_{mix}, is obtained from Equation 1.22 as

$$\Delta G_{\text{mix}} = RT(X_A \ln X_A + X_B \ln X_B) \tag{1.26}$$

Figure 1.9 shows ΔG_{mix} as a function of composition and temperature.

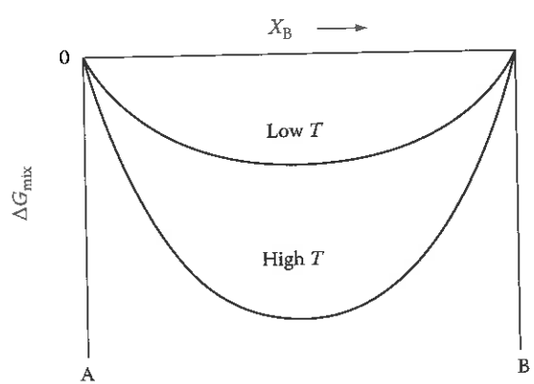

FIGURE 1.9
Free energy of mixing for an ideal solution.

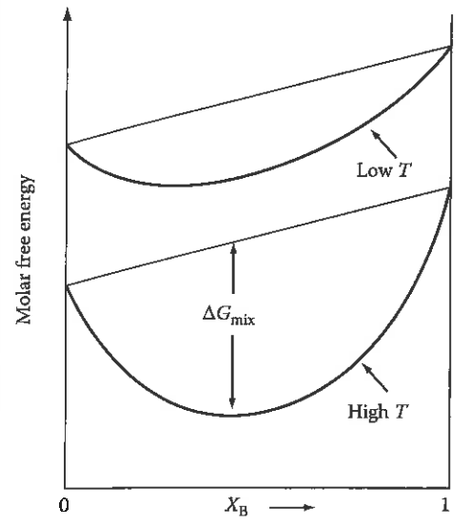

FIGURE 1.10
The molar free energy (free energy per mole of solution) for an ideal solid solution. A combination of Figures 1.8 and 1.9.

The actual free energy of the solution G will also depend on G_A and G_B. From Equations 1.19, 1.20, and 1.26

$$G = G_2 = X_A G_A + X_B G_B + RT(X_A \ln X_A + X_B \ln X_B) \tag{1.27}$$

This is shown schematically in Figure 1.10. Note that, as the temperature increases, G_A and G_B decrease and the free energy curves assume a greater curvature. The decrease in G_A and G_B is due to the thermal entropy of both components and is given by Equation 1.10.

It should be noted that all of the free energy–composition diagrams in this book are essentially schematic; if properly plotted the free energy curves must end asymptotically at the vertical axes of the pure components, i.e., tangential to the vertical axes of the diagrams. This can be shown by differentiating Equation 1.26 or Equation 1.27.

1.3.3 Chemical Potential

In alloys it is of interest to know how the free energy of a given phase will change when atoms are added or removed. If a small quantity of A, dn_A mol, is added to a large amount of a phase at constant temperature and pressure, the size of the system will increase by dn_A and therefore the total free energy of the system will also increase by a small amount dG'. If dn_A is small enough dG' will be proportional to the amount of A added. Thus we can write

$$dG' = \mu_A dn_A \ (T, P, n_B \text{ constant}) \tag{1.28}$$

The proportionality constant μ_A is called the partial molar free energy of A or alternatively the chemical potential of A in the phase. μ_A depends on the

composition of the phase, and therefore, dn_A must be so small that the composition is not significantly altered. If Equation 1.28 is rewritten it can be seen that a definition of the chemical potential of A is

$$\mu_A = \left(\frac{\partial G'}{\partial n_A}\right)_{T,P,n_B} \tag{1.29}$$

The symbol G' has been used for the Gibbs free energy to emphasize the fact that it refers to the whole system. The usual symbol G will be used to denote the molar free energy and is therefore independent of the size of the system.

Equations similar to Equations 1.28 and 1.29 can be written for the other components in the solution. For a binary solution at constant temperature and pressure the separate contributions can be summed:

$$dG' = \mu_A dn_A + \mu_B dn_B \tag{1.30}$$

This equation can be extended by adding further terms for solutions containing more than two components. If T and P changes are also allowed Equation 1.9 must be added giving the general equation

$$dG' = -SdT + VdP + \mu_A dn_A + \mu_B dn_B + \mu_C dn_C + \cdots$$

If 1 mol of the original phase contained X_A mol A and X_B mol B, the size of the system can be increased without altering its composition if A and B are added in the correct proportions, i.e., such that $dn_A{:}dn_B = X_A{:}X_B$. For example, if the phase contains twice as many A as B atoms ($X_A = 2/3$, $X_B = 1/3$) the composition can be maintained constant by adding two A atoms for every one B atom ($dn_A{:}dn_B = 2$). In this way, the size of the system can be increased by 1 mol without changing μ_A and μ_B. To do this X_A mol A and X_B mol B must be added and the free energy of the system will increase by the molar free energy G. Therefore from Equation 1.30

$$G = \mu_A X_A + \mu_B X_B \ (\text{J mol}^{-1}) \tag{1.31}$$

When G is known as a function of X_A and X_B, as in Figure 1.10 for example, μ_A and μ_B can be obtained by extrapolating the tangent to the G curve to the sides of the molar free energy diagram as shown in Figure 1.11. This can be obtained from Equations 1.30 and 1.31, remembering that $X_A + X_B = 1$, i.e., $dX_A = -dX_B$, and this is left as an exercise for the reader. It is clear from Figure 1.11 that μ_A and μ_B vary systematically with the composition of the phase.

Comparison of Equations 1.27 and 1.31 gives μ_A and μ_B for an ideal solution as

$$\begin{aligned} \mu_A &= G_A + RT \ln X_A \\ \mu_B &= G_B + RT \ln X_B \end{aligned} \tag{1.32}$$

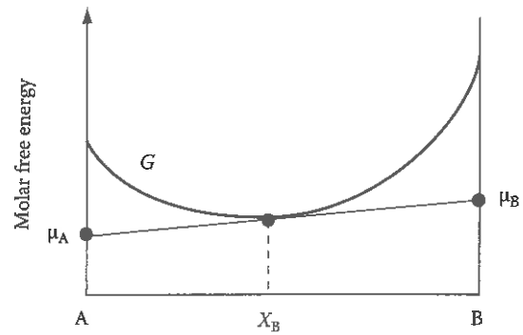

FIGURE 1.11
The relationship between the free energy curve for a solution and the chemical potentials of the components.

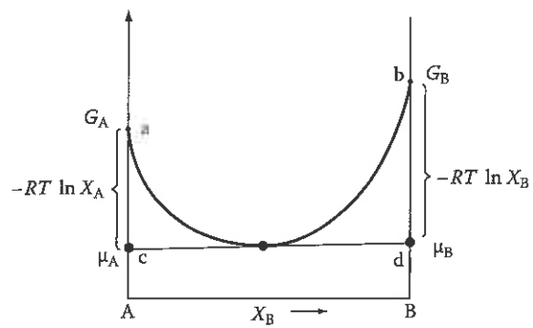

FIGURE 1.12
The relationship between the free energy curve and chemical potentials for an ideal solution.

which is a much simpler way of presenting Equation 1.27. These relationships are shown in Figure 1.12. The distances ac and bd are simply $-RT \ln X_A$ and $-RT \ln X_B$.

1.3.4 Regular Solutions

Returning to the model of a solid solution, so far it has been assumed that $\Delta H_{mix} = 0$; however, this type of behavior is exceptional in practice and usually mixing is endothermic (heat absorbed) or exothermic (heat evolved). The simple model used for an ideal solution can, however, be extended to include the ΔH_{mix} term by using the so-called quasichemical approach.

In the quasichemical model it is assumed that the heat of mixing, ΔH_{mix}, is only due to the bond energies between adjacent atoms. For this assumption to be valid it is necessary that the volumes of pure A and B are equal and do not change during mixing so that the interatomic distance and bond energies are independent of composition.

The structure of an ordinary solid solution is shown schematically in Figure 1.13. Three types of interatomic bonds are present:

1. A–A bonds each with an energy ε_{AA}
2. B–B bonds each with an energy ε_{BB}
3. A–B bonds each with an energy ε_{AB}

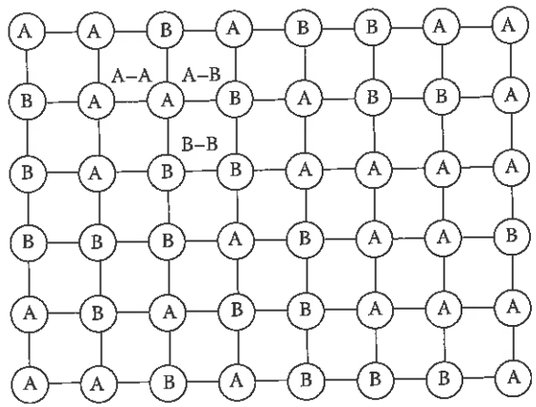

FIGURE 1.13
Different types of interatomic bond in solid solution.

By considering zero energy to be the state where the atoms are separated to infinity ε_{AA}, ε_{BB}, and ε_{AB} are negative quantities, and become increasingly more negative as the bonds become stronger. The internal energy of the solution E will depend on the number of bonds of each type P_{AA}, P_{BB}, and P_{AB} such that

$$E = P_{AA}\varepsilon_{AA} + P_{BB}\varepsilon_{BB} + P_{AB}\varepsilon_{AB}$$

Before mixing pure A and B contain only A–A and B–B bonds, respectively, and by considering the relationships between P_{AA}, P_{BB}, and P_{AB} in the solution it can be shown[1] that the change in internal energy on mixing is given by

$$\Delta H_{mix} = P_{AB}\varepsilon \tag{1.33}$$

where

$$\varepsilon = \varepsilon_{AB} - \frac{1}{2}(\varepsilon_{AA} + \varepsilon_{BB}) \tag{1.34}$$

that is, ε is the difference between the A–B bond energy and the average of the A–A and B–B bond energies.

If $\varepsilon = 0$, $\Delta H_{mix} = 0$ and the solution is ideal, as considered in Section 1.3.2. In this case, the atoms are completely randomly arranged and the entropy of mixing is given by Equation 1.25. In such a solution it can also be shown[1] that

$$P_{AB} = N_a z X_A X_B \text{ (bonds mol}^{-1}\text{)} \tag{1.35}$$

where
N_a is Avogadro's number
z is the number of bonds per atom

If $\varepsilon < 0$ the atoms in the solution will prefer to be surrounded by atoms of the opposite type and this will increase P_{AB}, whereas, if $\varepsilon > 0$, P_{AB} will tend to be less than in a random solution. However, provided ε is not too different from zero, Equation 1.35 is still a good approximation in which case

$$\Delta H_{mix} = \Omega X_A X_B \tag{1.36}$$

where

$$\Omega = N_a z \varepsilon \tag{1.37}$$

Real solutions that closely obey Equation 1.36 are known as regular solutions. The variation of ΔH_{mix} composition is parabolic and is shown in Figure 1.14 for $\Omega > 0$. Note that the tangents at $X_A = 0$ and 1 are related to Ω as shown.

The free energy change on mixing a regular solution is given by Equations 1.21, 1.25, and 1.36 as

$$\Delta G_{mix} = \underbrace{\Omega X_A X_B}_{\Delta H_{mix}} + \underbrace{RT(X_{mix} \ln X_A + X_B \ln X_B)}_{-T\Delta S_{mix}} \tag{1.38}$$

This is shown in Figure 1.15 for different values of Ω and temperature. For exothermic solutions $\Delta H_{mix} < 0$ and mixing results in a free energy decrease at all temperatures (Figure 1.15a and b). When $\Delta H_{mix} > 0$, however, the situation is more complicated. At high temperatures $T\Delta S_{mix}$ is greater than ΔH_{mix} for all compositions and the free energy curve has a positive curvature at all points (Figure 1.15c). At low temperatures, on the other hand, $T\Delta S_{mix}$ is smaller and ΔG_{mix} develops a negative curvature in the middle (Figure 1.15d).

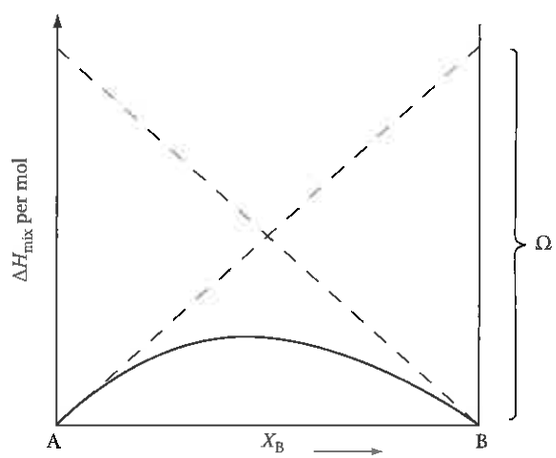

FIGURE 1.14
The variation of ΔH_{mix} with composition for a regular solution.

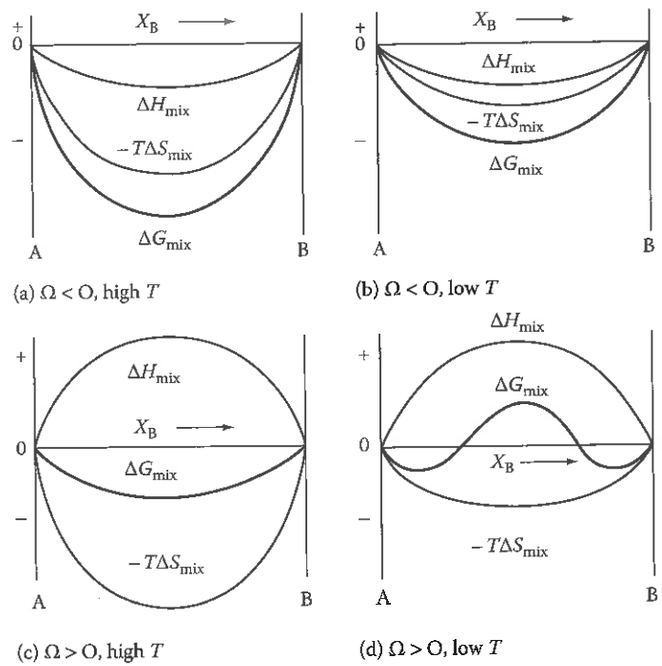

FIGURE 1.15
The effect of ΔH_{mix} and T on ΔG_{mix}.

Differentiating Equation 1.25 shows that, as X_A or $X_B \to 0$, the $-T\Delta S_{mix}$ curve becomes vertical whereas the slope of the ΔH_{mix} curve tends to a finite value Ω (Figure 1.14). This means that, except at absolute zero, ΔG_{mix} always decreases on addition of a small amount of solute.

The actual free energy of the alloy depends on the values chosen for G_A and G_B and is given by Equations 1.19, 1.20, and 1.38 as

$$G = X_A G_A + X_B G_B + \Omega X_A X_B + RT(X_A \ln X_A + X_B \ln X_B) \tag{1.39}$$

This is shown in Figure 1.16 along with the chemical potentials of A and B in the solution. Using the relationship $X_A X_B = X_A^2 X_B + X_B^2 X_A$ and comparing Equations 1.31 and 1.39 shows that for a regular solution

$$\mu_A = G_A + \Omega(1 - X_A)^2 + RT \ln X_A \tag{1.40}$$

and

$$\mu_B = G_B + \Omega(1 - X_B)^2 + RT \ln X_B$$

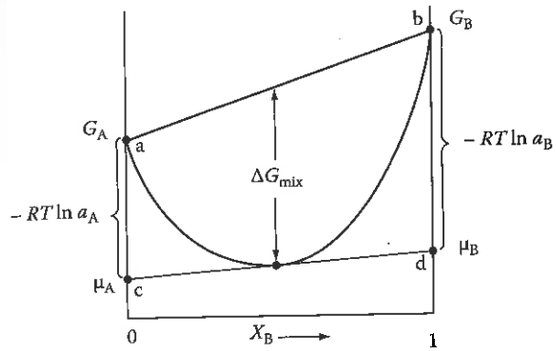

FIGURE 1.16
The relationship between molar free energy and activity.

1.3.5 Activity

Equation 1.32 for the chemical potential of an ideal alloy was simple and it is convenient to retain a similar expression for any solution. This can be done by defining the activity of a component, a, such that the distances ac and bd in Figure 1.16 are $-RT \ln a_A$ and $-RT \ln a_B$. In this case,

$$\mu_A = G_A + RT \ln a_A \tag{1.41}$$

and

$$\mu_B = G_B + RT \ln a_B$$

In general a_A and a_B will be different from X_A and X_B and the relationship between them will vary with the composition of the solution. For a regular solution, comparison of Equations 1.40 and 1.41 gives

$$\ln\left(\frac{a_A}{X_A}\right) = \frac{\Omega}{RT}(1 - X_A)^2 \tag{1.42}$$

and

$$\ln\left(\frac{a_B}{X_B}\right) = \frac{\Omega}{RT}(1 - X_B)^2$$

Assuming pure A and pure B have the same crystal structure, the relationship between a and X for any solution can be represented graphically as illustrated in Figure 1.17. Line 1 represents an ideal solution for which $a_A = X_A$ and $a_B = X_B$. If $\Delta H_{mix} < 0$ the activity of the components in solution will be less in an ideal solution (line 2) and vice versa when $\Delta H_{mix} > 0$ (line 3).

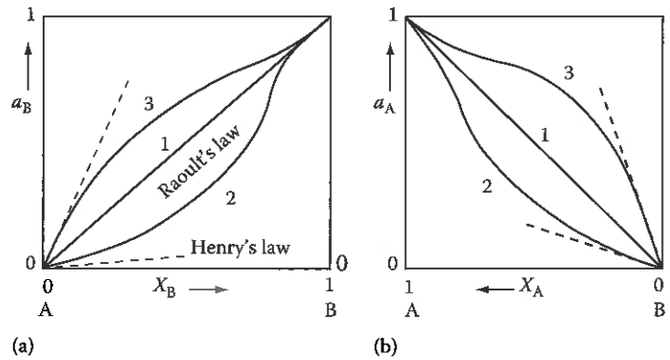

FIGURE 1.17
The variation of activity with composition (a) a_B (b) a_A. Line 1, ideal solution (Raoult's law); line 2, $\Delta H_{mix} < 0$; line 3, $\Delta H_{mix} > 0$.

The ratio (a_A/X_A) is usually referred to as γ_A, the activity coefficient of A, that is

$$\gamma_A = a_A/X_A \tag{1.43}$$

For a dilute solution of B in A, Equation 1.42 can be simplified by letting $X_B \rightarrow 0$ in which case,

$$\gamma_B = \frac{a_B}{X_B} \simeq \text{constant (Henry's law)} \tag{1.44}$$

and

$$\gamma_A = \frac{a_A}{X_A} \simeq 1 \text{ (Raoult's law)} \tag{1.45}$$

Equation 1.44 is known as Henry's law and Equation 1.45 as Raoult's law; they apply to all solutions when sufficiently dilute.

Since activity is simply related to chemical potential via Equation 1.41 the activity of a component is just another means of describing the state of the component in a solution. No extra information is supplied and its use is simply a matter of convenience as it often leads to simpler mathematics.

Activity and chemical potential are simply a measure of the tendency of the atom to leave a solution. If the activity or chemical potential is low the atoms are reluctant to leave the solution which means, for example, that the vapor pressure of the component in equilibrium with the solution will be relatively low. It will also be apparent later that the activity or chemical potential of a component is important when several condensed phases are in equilibrium.

1.3.6 Real Solutions

While the previous model provides a useful description of the effects of configurational entropy and interatomic bonding on the free energy of binary solutions its practical use is rather limited. For many systems the model is an oversimplification of reality and does not predict the correct dependence of ΔG_{mix} on composition and temperature.

As already indicated, in alloys where the enthalpy of mixing is not zero (ε and $\Omega \neq 0$) the assumption that a random arrangement of atoms is the equilibrium, or most stable arrangement is not true, and the calculated value for ΔG_{mix} will not give the minimum free energy. The actual arrangement of atoms will be a compromise that gives that lowest internal energy consistent with sufficient entropy, or randomness, to achieve the minimum free energy. In systems with $\varepsilon < 0$ the internal energy of the system is reduced by increasing the number of A–B bonds, i.e., by ordering the atoms as shown in Figure 1.18a. If $\varepsilon > 0$ the internal energy can be reduced by increasing the number of A–A and B–B bonds, i.e., by the clustering of the atoms into A-rich and B-rich groups (Figure 1.18b). However, the degree of ordering or clustering will decrease as temperature increases due to the increasing importance of entropy.

In systems where there is a size difference between the atoms the quasi-chemical model will underestimate the change in internal energy on mixing since no account is taken of the elastic strain fields which introduce a strain energy term into ΔH_{mix}. When the size difference is large this effect can dominate over the chemical term.

When the size difference between the atoms is very large then interstitial solid solutions are energetically most favorable (Figure 1.18c). New mathematical models are needed to describe these solutions.

In systems where there is a strong chemical bonding between the atoms there is a tendency for the formation of intermetallic phases. These are distinct from solutions based on the pure components since they have

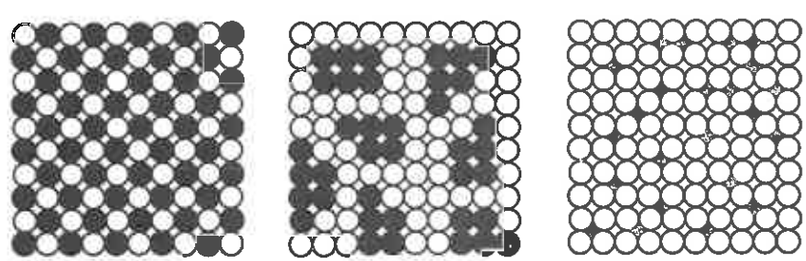

FIGURE 1.18
Schematic representation of solid solutions: (a) ordered substitutional, (b) clustering, and (c) random interstitial.

a different crystal structure and may also be highly ordered. Intermediate phases and ordered phases are discussed further in the next two sections.

1.3.7 Ordered Phases

If the atoms in a substitutional solid solution are completely randomly arranged each atom position is equivalent and the probability that any given site in the lattice will contain an A atom will be equal to the fraction of A atoms in the solution X_A, similarly X_B for the B atoms. In such solutions P_{AB}, the number of A–B bonds, is given by Equation 1.35. If $\Omega < 0$ and the number of A–B bonds is greater than this, the solution is said to contain short-range order (SRO). The degree of ordering can be quantified by defining a SRO parameter s such that

$$s = \frac{P_{AB} - P_{AB}(\text{random})}{P_{AB}(\text{max}) - P_{AB}(\text{random})}$$

where $P_{AB}(\text{max})$ and $P_{AB}(\text{random})$ refer to the maximum number of bonds possible and the number of bonds for a random solution, respectively. Figure 1.19 illustrates the difference between random and short-range ordered solutions.

In solutions with compositions that are close to a simple ratio of A:B atoms another type of order can be found as shown schematically in Figure 1.18a. This is known as long-range order (LRO). Now the atom sites are no longer equivalent but can be labeled as A-sites and B-sites. Such a solution can be considered to be a different (ordered) phase separate from the random or nearly random solution.

Consider Cu–Au alloys as a specific example. Cu and Au are both fcc and totally miscible. At high temperatures Cu or Au atoms can occupy any site

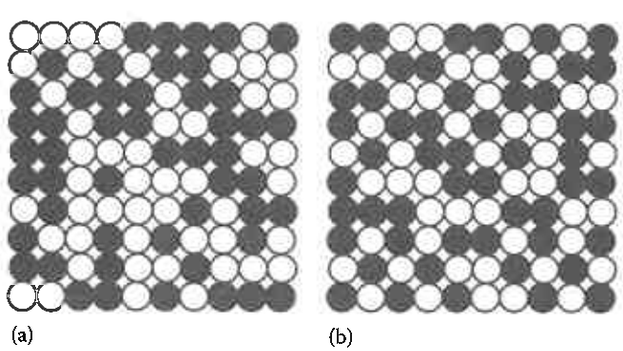

FIGURE 1.19
(a) Random A–B solution with total of 100 atoms and $X_A = X_B = 0.5$. $P_{AB} \sim 100$, $S = 0$. (b) Same alloy with SRO $P_{AB} = 132$. $P_{AB(max)} \sim 200$, $S = (132 - 100)/(200 - 100) = 0.32$.

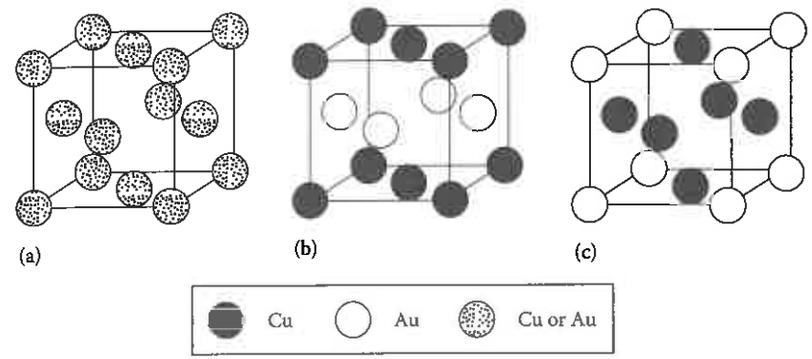

FIGURE 1.20
Ordered substitutional structures in the Cu–Au system: (a) high-temperature disordered structure, (b) CuAu superlattice, and (c) Cu_3Au superlattice.

and the lattice can be considered as fcc with a "random" atom at each lattice point as shown in Figure 1.20a. At low temperatures, however, solutions with $X_{Cu} = X_{Au} = 0.5$, i.e., a 50/50 Cu/Au mixture, form an ordered structure in which the Cu and Au atoms are arranged in alternate layers (Figure 1.20b). Each atom position is no longer equivalent and the lattice is described as a CuAu superlattice. In alloys with the composition Cu_3Au another superlattice is found (Figure 1.20c).

The entropy of mixing of structures with LRO is extremely small and with increasing temperature the degree order decreases until above some critical temperature there is no LRO at all. This temperature is a maximum when the composition is the ideal required for the superlattice. However, LRO can still be obtained when the composition deviates from the ideal if some of the atom sites are left vacant of if some atoms sit on wrong sites. In such cases it can be easier to disrupt the order with increasing temperature and critical temperature is lower (Figure 1.21).

The most common ordered lattices in other systems are summarized in Figure 1.22 along with their Structurbericht notation and examples of alloys

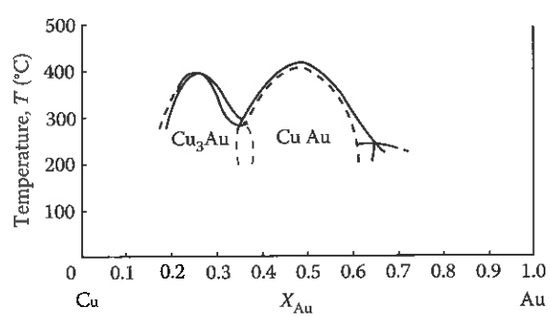

FIGURE 1.21
Part of the Cu–Au phase diagram showing the regions where the Cu_3Au and CuAu superlattices are stable.

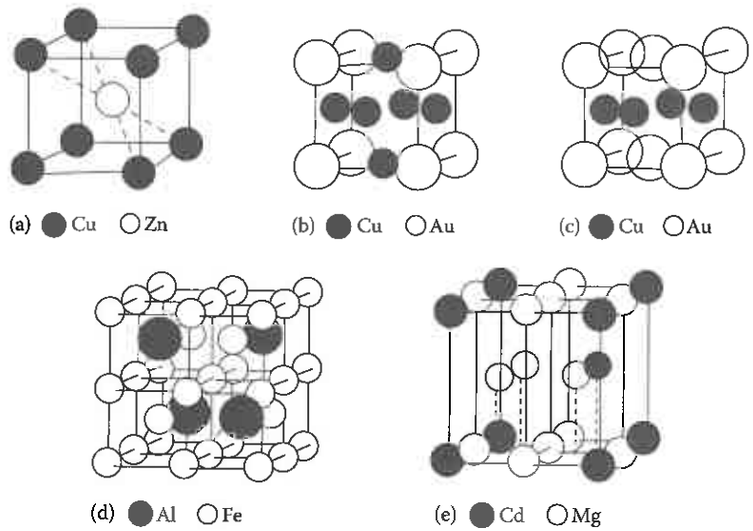

FIGURE 1.22
The five common ordered lattices, examples of which are (a) $L2_0$: CuZn, FeCo, NiAl, FeAl, AgMg; (b) $L1_2$: Cu_3Au, Au_3Cu, Ni_3Mn, Ni_3Fe, Ni_3Al, Pt_3Fe; (c) $L1_0$: CuAu, CoPt, FePt; (d) $D0_3$: Fe_3Al, Fe_3Si, Fe3Be, Cu_3Al; (e) $D0_{19}$: Mg_3Cd, Cd_3Mg, Ti_3Al, Ni_3Sn. (After Smallman, R.E., *Modern Physical Metallurgy*, 3rd edn., Butterworths, London, 1970.)

in which they are found. Finally, note that the critical temperature for loss of LRO increases with increasing Ω, or ΔH_{mix}, and in many systems the ordered phase is stable up to the melting point.

1.3.8 Intermediate Phases

Often the configuration of atoms that has the minimum free energy after mixing does not have the same crystal structure as either of the pure components. In such cases the new structure is known as an intermediate phase.

Intermediate phases are often based on an ideal atom ratio that results in a minimum Gibbs free energy. For compositions that deviate from the ideal, the free energy is higher giving a characteristic "U" shape to the G curve, as in Figure 1.23. The range of compositions over which the free energy curve has a meaningful existence depends on the structure of the phase and the type of interatomic bonding—metallic, covalent, or ionic. When small composition deviations cause a rapid rise in G the phase is referred to as an intermetallic compound and is usually stoichiometric, i.e., has a formula A_mB_n where m and n are integers (Figure 1.23a). In other structures fluctuations in composition can be tolerated by some atoms occupying "wrong" positions or by atom sites being left vacant, and in these cases the curvature of the G curve is much less (Figure 1.23b).

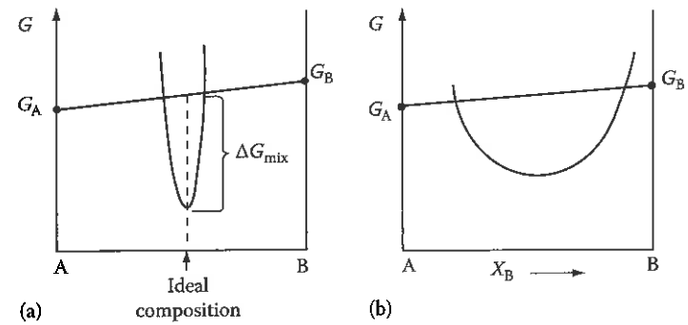

FIGURE 1.23
Free energy curves for intermediate phases: (a) for an intermetallic compound with a very narrow stability range, (b) for an intermediate phase with a wide stability range.

Some intermediate phases can undergo order–disorder transformations in which an almost random arrangement of the atoms is stable at high temperatures and an ordered structure is stable below some critical temperature. Such a transformation occurs in the β-phase in the Cu–Zn system for example (see Section 5.10).

The structure of intermediate phases is determined by three main factors: relative atomic size, valency, and electronegativity. When the component atoms differ in size by a factor of about 1.1–1.6 it is possible for the atoms to fill space most efficiently if the atoms order themselves into one of the so-called Laves phases based on $MgCu_2$, $MgZn_2$, and $MgNi_2$ (Figure 1.24). Another example where atomic size determines the structure is in the formation of the interstitial compounds MX, M_2X, MX_2, and M_6X where M can be Zr, Ti, V, Cr, etc. and X can be H, B, C, and N. In this case, the M atoms form a

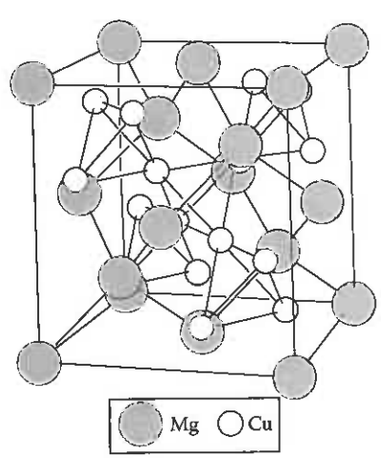

FIGURE 1.24
Structure of $MgCu_2$ (A Laves phase). (From Wernick, J.H., in *Physical Metallurgy*, 2nd edn., Chapter 5, Cahn, R.W. (Ed.), North Holland, Amsterdam, 1974. With permission.)

cubic or hcp arrangement and the X atoms are small enough to fit into the interstices between them.

The relative valency of the atoms becomes important in the so-called electron phases, e.g., α and β phases. The free energy of these phases depends on the number of valency electrons per unit cell, and this varies with composition due to the valency difference.

The electronegativity of an atom is a measure of how strongly it attracts electrons and in systems where the two components have very different electronegativities ionic bonds can be formed producing normal valency compounds, e.g., Mg^{2+} and Sn^{4-} are ionically bonded in Mg_2Sn.[2]

1.4 Equilibrium in Heterogeneous Systems

It is usually the case that A and B do not have the same crystal structure in their pure states at a given temperature. In such cases two free energy curves must be drawn, one for each structure. The stable forms of pure A and B at a given temperature (and pressure) can be denoted as α and β, respectively. For the sake of illustration let α be fcc and β bcc. The molar free energies of fcc A and bcc B are shown in Figure 1.25a as points a and b. The first step in drawing the free energy curve of the fcc α-phase is, therefore, to convert the stable bcc arrangement of B atoms into an unstable fcc arrangement. This requires an increase in free energy, bc. The free energy curve for the α-phase can now be constructed as before by mixing fcc A and fcc B as shown in Figure 1.25. $-\Delta G_{mix}$ for α of composition X is given by the distance de as usual.

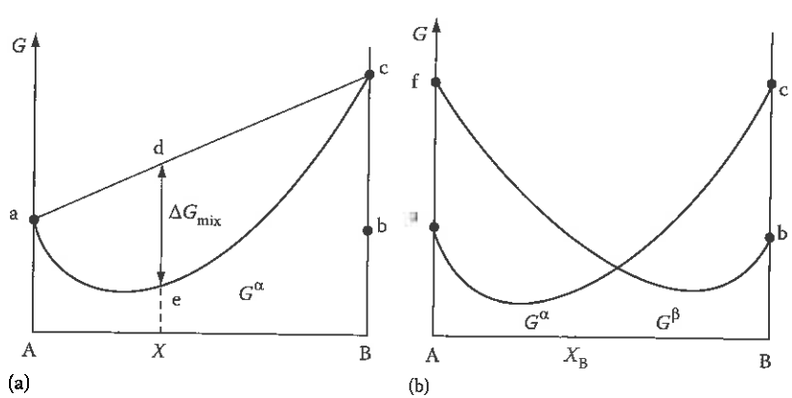

FIGURE 1.25
(a) Molar free energy curve for the α-phase. (b) Molar free energy curves for α- and β-phases.

A similar procedure produces the molar free energy curve for the β-phase (Figure 1.25b). The distance af is now the difference in free energy between bcc A and fcc A.

It is clear from Figure 1.25b that A-rich alloys will have the lowest free energy as a homogeneous α-phase and B-rich alloys as β-phase. For alloys with compositions near the cross-over in G curves the situation is not so straightforward. In this case, it can be shown that the total free energy can be minimized by the atoms separating into two phases.

It is first necessary to consider a general property of molar free energy diagrams when phase mixtures are present. Suppose an alloy consists of two phases α and β each of which has a molar free energy given by G^α and G^β (Figure 1.26). If the overall composition of the phase mixture is X_B^0 the lever rule gives the relative number of moles of α and β that must be present, and the molar free energy of the phase mixture G is given by the point on the straight line between α and β as shown in the figure. This result can be proven most readily using the geometry of Figure 1.26. The lengths ad and cf, respectively, represents the molar free energies of the α- and β-phases present in the alloy. Point g is obtained by the intersection of be and dc so that bcg and acd, as well as deg and dfc, form similar triangles. Therefore, $bg/ad = bc/ac$ and $ge/cf = ab/ac$. According to the lever rule, 1 mol of alloy will contain bc/ac mol of α and ab/ac mol of β. It follows that bg and ge represent the separate contributions from the α- and β-phases to the total free energy of 1 mol of alloy. Therefore, the length be represents the molar free energy of the phase mixture.

Consider now alloy X^0 in Figure 1.27a. If the atoms are arranged as a homogeneous phase, the free energy will be lowest as α, i.e., G_0^α per mole. However, from the above it is clear that the system can lower its free energy if the atoms separate into two phases with compositions α_1 and β_1 for example. The free energy of the system will then be reduced to G_1. Further reductions in free energy can be achieved if the A and B atoms interchange between the α- and β-phases until the compositions α_e and β_e are reached (Figure 1.27b). The free energy of the system G_e is now a minimum and there is no desire for further change. Consequently the system is in equilibrium and α_e and β_e are the equilibrium compositions of the α- and β-phases.

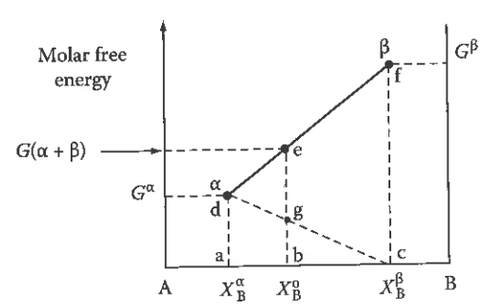

FIGURE 1.26
The molar free energy of a two-phase mixture (α + β).

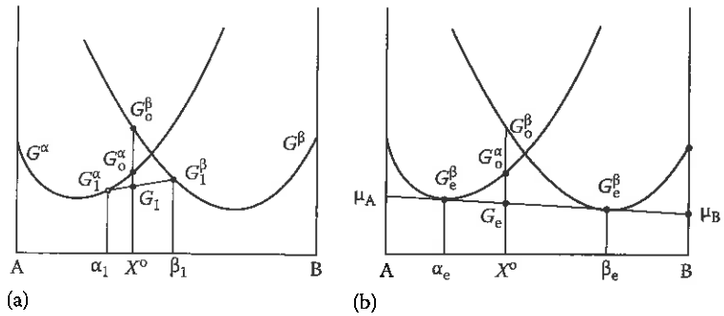

FIGURE 1.27
(a) Alloy X^0 has a free energy G_1 as a mixture of $\alpha_1 + \beta_1$. (b) At equilibrium, alloy X^0 has a minimum free energy G_e when it is a mixture of $\alpha_e + \beta_e$.

This result is quite general and applies to any alloy with an overall composition between α_e and β_e: only the relative amounts of the two phases change, as given by the lever rule. When the alloy composition lies outside this range, however, the minimum free energy lies on the G^α or G^β curves and the equilibrium state of the alloy is a homogeneous single phase.

From Figure 1.27 it can be seen that equilibrium between two phases requires that the tangents to each G curve at the equilibrium compositions lie on a common line. In other words, each component must have the same chemical potential in the phased, i.e., for heterogeneous equilibrium:

$$\mu_A^\alpha = \mu_A^\beta, \quad \mu_\beta^\alpha = \mu_B^\beta \tag{1.46}$$

The condition for equilibrium in a heterogeneous system containing two phases can also be expressed using the activity concept defined for homogeneous systems in Figure 1.16. In heterogeneous systems containing more than one phase the pure components can, at least theoretically, exist in different crystal structures. The most stable state, with the lowest free energy, is usually defined as the state in which the pure component has unit activity. In the present example this would correspond to defining the activity of A in pure α-A as unity, i.e., when $X_A = 1$, $a_A^\alpha = 1$. Similarly when $X_B = 1$, $a_B^\beta = 1$. This definition of activity is shown graphically in Figure 1.28a; Figure 1.28b and c shows how the activities of B and A vary with the composition of the α- and β-phases. Between A and α_e, and β_e and B, where single phases are stable, the activities (or chemical potentials) vary and for simplicity ideal solutions have been assumed in which case there is a straight line relationship between a and X. Between α_e and β_e the phase compositions in equilibrium do not change and the activities are equal and given by points q and r. In other words, when two phases exist in equilibrium, the activities of the components in the system must be equal in the two phases, i.e.,

$$a_A^\alpha = a_A^\beta, \quad a_B^\alpha = a_B^\beta \tag{1.47}$$

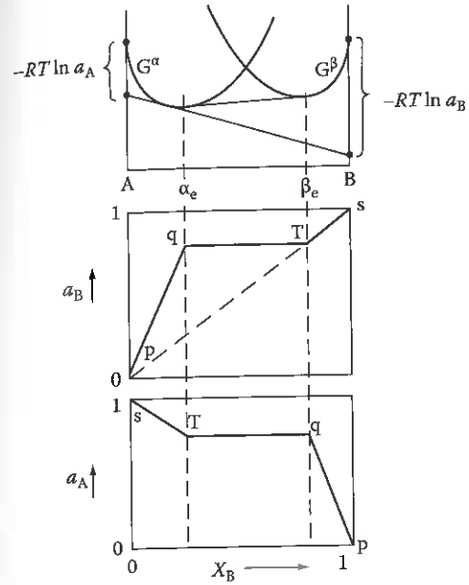

FIGURE 1.28
The variation of a_A and a_B with composition for a binary system containing two ideal solutions, α and β.

1.5 Binary Phase Diagrams

In Section 1.4, it has been shown how the equilibrium state of an alloy can be obtained from the free energy curves at a given temperature. The next step is to see how equilibrium is affected by temperature.

1.5.1 Simple Phase Diagram

The simplest case to start with is when A and B are completely miscible in both the solid and liquid states and both are ideal solutions. The free energy of pure A and pure B will vary with temperature as shown schematically in Figure 1.4. The equilibrium melting temperatures of the pure components occur when $G^S = G^L$, i.e., at $T_m(A)$ and $T_m(B)$. The free energy of both phases decreases as temperature increases. These variations are important for A–B alloys also since they determine the relative positions of G_A^S, G_A^L, G_B^S, and G_B^L on the molar free energy diagrams of the alloy at different temperatures (Figure 1.29).

At a high temperature $T_1 > T_m(A) > T_m(B)$ the liquid will be the stable phase for pure A and pure B, and for the simple case we are considering that the liquid also has a lower free energy than the solid at all the intermediate compositions as shown in Figure 1.29a.

Decreasing the temperature will have two effects: first G_A^L and G_B^L will increase more rapidly than G_A^S and G_B^S, second the curvature of the G

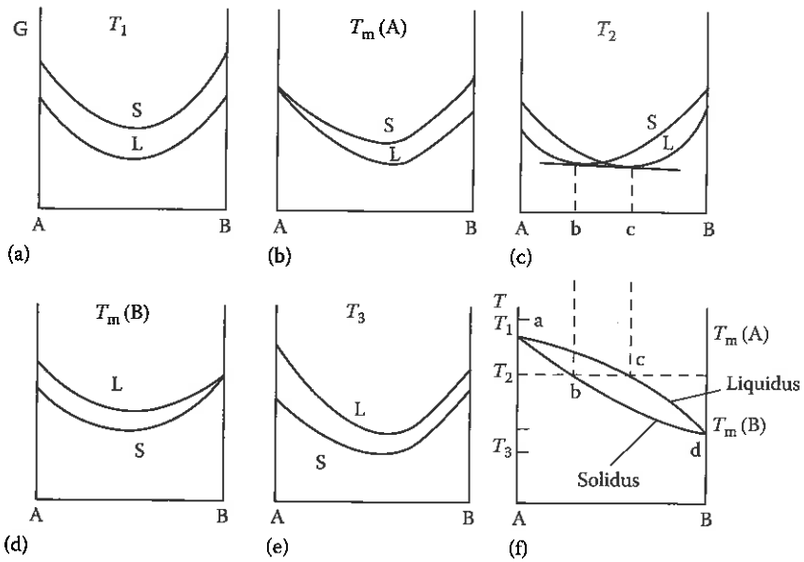

FIGURE 1.29
Derivation of a simple phase diagram from the free energy curves for the liquid (L) and solid (S).

curves will be reduced due to the smaller contribution of $-T\Delta S_{mix}$ to the free energy.

At T_m(A), Figure 1.29b, $G_A^S = G_A^L$, and this corresponds to point a on the A–B phase diagram, Figure 1.29f. At a lower temperature T_2 the free energy curves cross, Figure 1.29c, and common tangent construction indicates that alloys between A and b are solid at equilibrium, between c and B they are liquid, and between b and c equilibrium consists of a two-phase mixture (S + L) with compositions b and c. These points are plotted on the equilibrium phase diagram at T_2.

Between T_2 and T_m(B) G^L continues to rise faster than G^S so that points b and c in Figure 1.29c will both move to the right tracing out the solidus and liquidus lines in the phase diagram. Eventually the T_m(B) b and c will meet at a single point, d in Figure 1.29f. Below T_m(B) the free energy of the solid phase is everywhere below that of the liquid and all alloys are stable as a single-phase solid.

1.5.2 Systems with a Miscibility Gap

Figure 1.30 shows the free energy curves for a system in which the liquid phase is approximately ideal, but for the solid phase $\Delta H_{mix} > 0$, i.e., the A and B atoms dislike each other. Therefore, at low temperatures (T_3) the free energy curve for the solid assumes a negative curvature in the middle, Figure 1.30c, and the solid solution is most stable as a mixture of two phases α' and α''

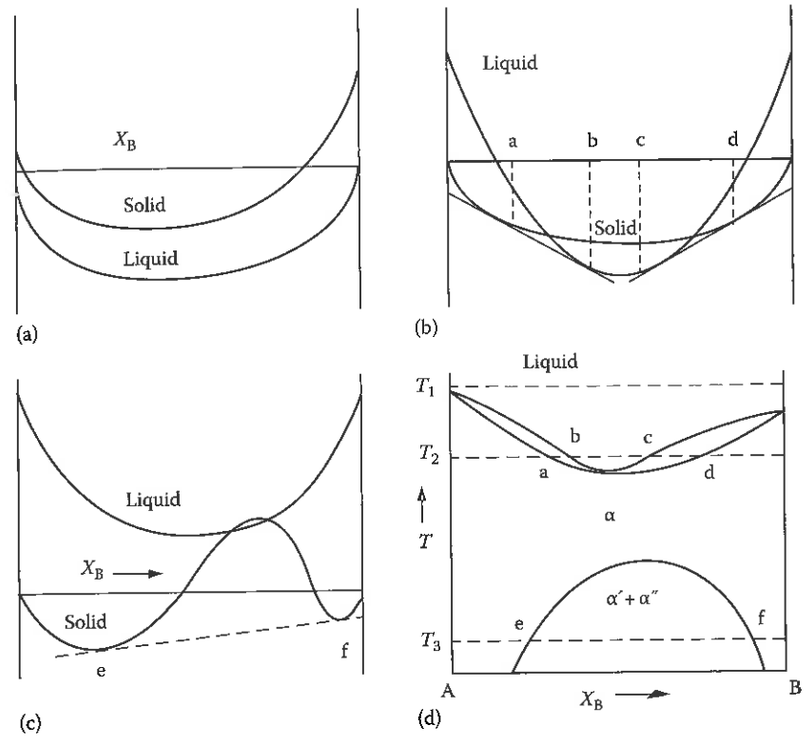

FIGURE 1.30
Derivation of a phase diagram (d) where $\Delta H_{mix}^S > \Delta H_{mix}^L = 0$. Free energy versus composition curves for (a) T_1, (b) T_2, and (c) T_3.

with composition e and f. At higher temperatures, when $-T\Delta S_{mix}$ becomes larger, e and f approach each other and eventually disappear as shown in the phase diagram (Figure 1.30d). The $\alpha' + \alpha''$ region is known as the miscibility gap.

The effect of a positive ΔH_{mix} in the solid is already apparent at higher temperatures where it gives rise to a minimum melting point mixture. The reason why all alloys should melt at temperatures below the melting points of both components can be qualitatively understood since the atoms in the alloy repel each other making the disruption of the solid into a liquid phase possible at lower temperatures than in either pure A or pure B.

1.5.3 Ordered Alloys

The opposite type of effect arises when $\Delta H_{mix} < 0$. In these systems melting will be more difficult in the alloys and a maximum melting point mixture may appear. This type of alloy also has a tendency to order at low temperatures as shown in Figure 1.31a. If the attraction between unlike atoms is very strong the ordered phase may extend as far as the liquid (Figure 1.31b).

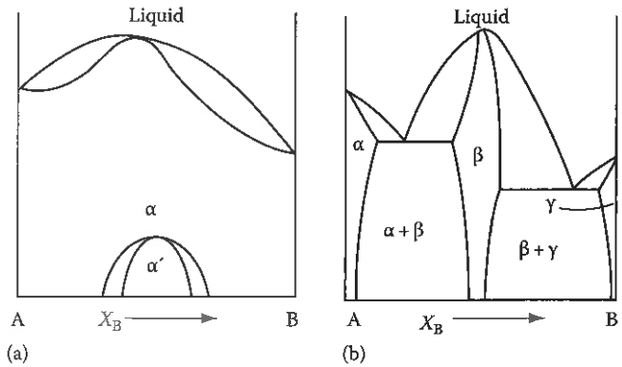

FIGURE 1.31
(a) Phase diagram when $\Delta H^S_{mix} < 0$; (b) as (a) but even more negative ΔH^S_{mix}. (After Swalin, R.A., *Thermodynamics of Solids*, Wiley, New York, 1972.)

1.5.4 Simple Eutectic Systems

If ΔH^S_{mix} is much larger than zero the miscibility gap in Figure 1.30d can extend into the liquid phase. In this case, a simple eutectic phase diagram results as shown in Figure 1.32. A similar phase diagram can result when A and B have different crystal structures as illustrated in Figure 1.33.

1.5.5 Phase Diagrams Containing Intermediate Phases

When stable intermediate phases can form, extra free energy curves appear in the phase diagram. An example is shown in Figure 1.34, which also illustrates how a peritectic transformation is related to the free energy curves.

An interesting result of the common tangent construction is that the stable composition range of the phase in the phase diagram need not include the composition with the minimum free energy, but is determined by the relative free energies of adjacent phases (Figure 1.35). This can explain why the composition of the equilibrium phase appears to deviate from that which would be predicated from the crystal structure. For example, the θ-phase in the Cu–Al system is usually denoted as $CuAl_2$ although the composition $X_{Cu} = 1/3$, $X_{Al} = 2/3$ is not covered by the θ field on the phase diagram.

1.5.6 Gibbs Phase Rule

The condition for equilibrium in a binary system containing two phases is given by Equation 1.46 or Equation 1.47. A more general requirement for systems containing several components and phases is that the chemical potential of each component must be identical in every phase, i.e.,

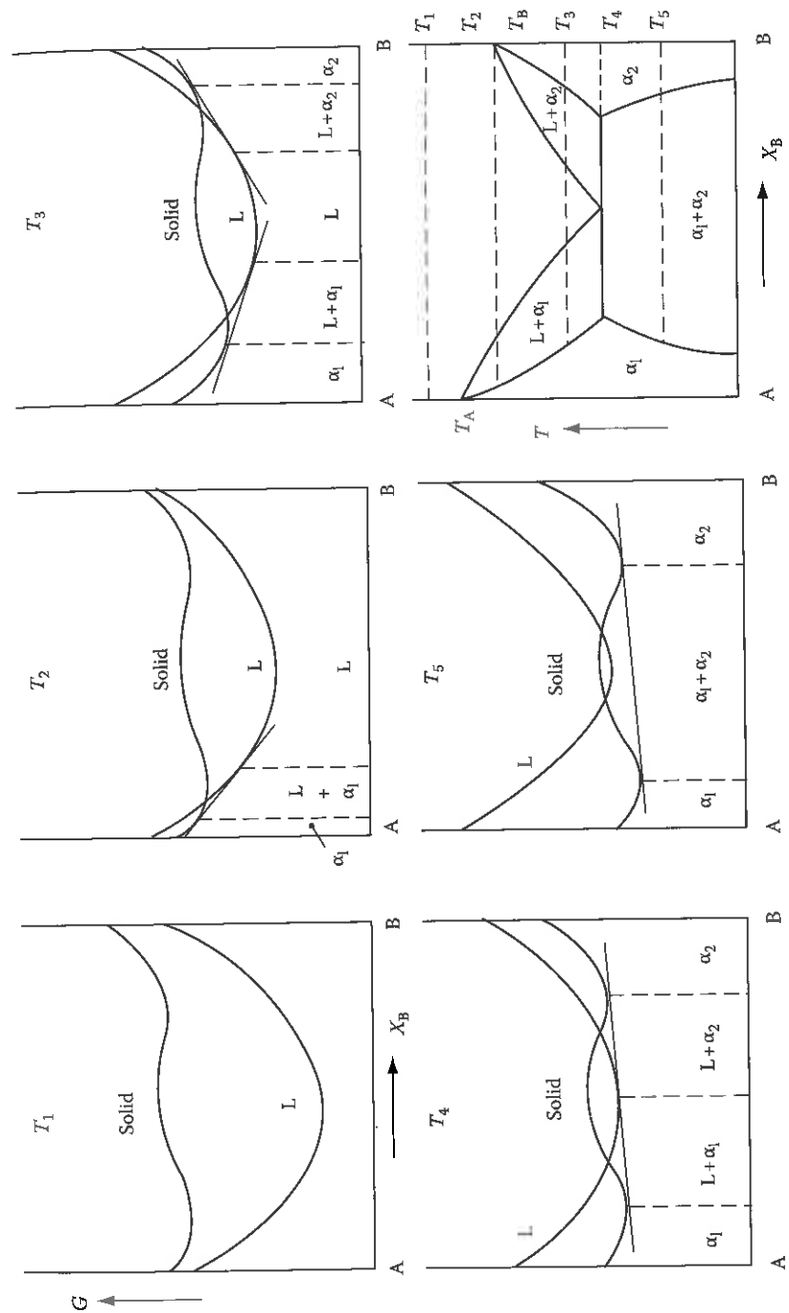

FIGURE 1.32
Derivation of a eutectic phase diagram where both solid phases have the same crystal structure. (After Cottrell, A.H., *Theoretical Structural Metallurgy*, Edward Arnold, London, 1995.)

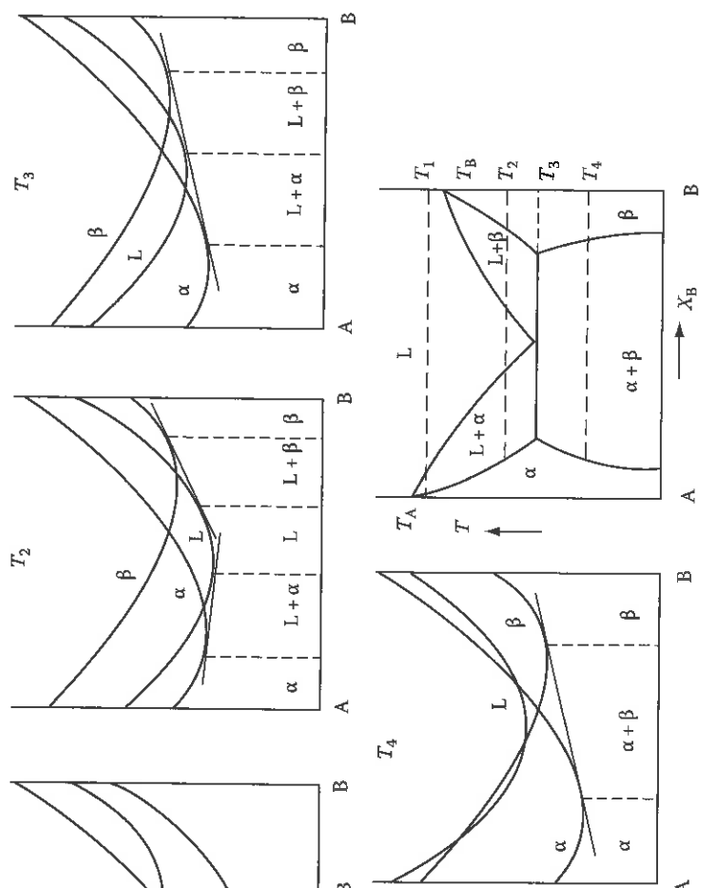

FIGURE 1.33
Derivation of a eutectic phase diagram where each solid phase has a different crystal structure. (After Prince, A., *Alloy Phase Equilibria*, Elsevier, Amsterdam, 1966.)

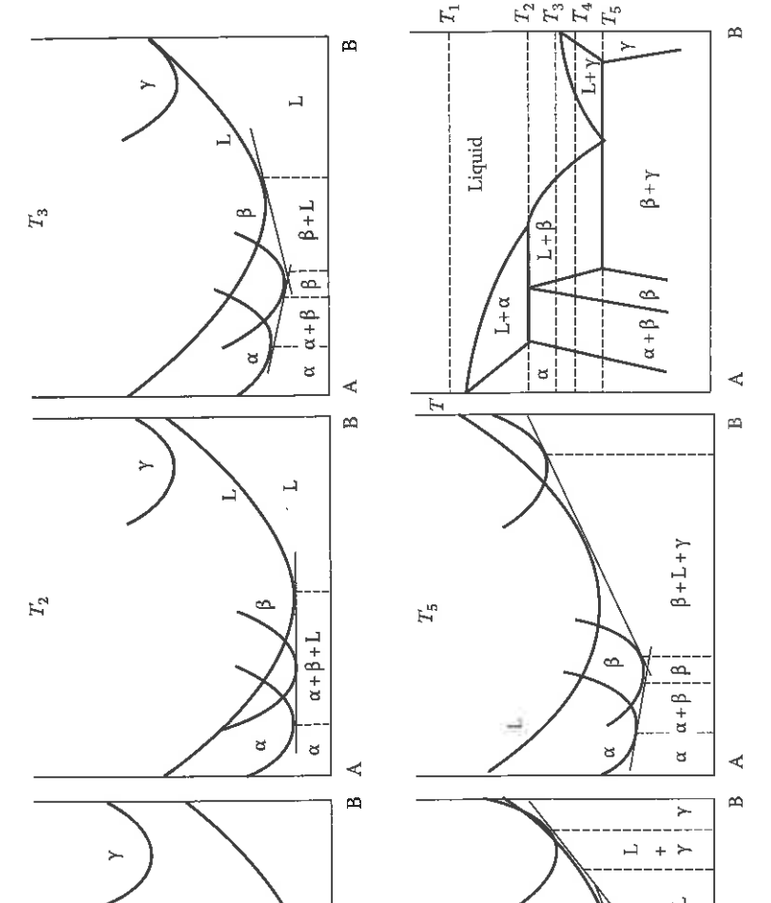

FIGURE 1.34
Derivation of a complex phase diagram. (After Cottrell, A.H., *Theoretical Structural Metallurgy*, Edward Arnold, London, 1955.)

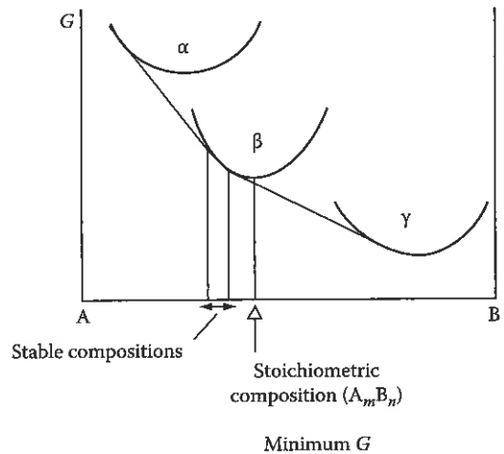

FIGURE 1.35
Free energy diagram to illustrate that the range of compositions over which a phase is stable depends on the free energies of the other phases in equilibrium.

$$\mu_A^\alpha = \mu_A^\beta = \mu_A^\gamma = \cdots$$
$$\mu_B^\alpha = \mu_B^\beta = \mu_B^\gamma = \cdots \tag{1.48}$$
$$\mu_C^\alpha = \mu_C^\beta = \mu_C^\gamma = \cdots$$

The proof of this relationship is left as an exercise for the reader (see Exercise 1.10). A consequence of this general condition is the Gibbs phase rule. This states that if a system containing C components and P phases is in equilibrium the number of degrees of freedom F is given by

$$P + F = C + 2 \tag{1.49}$$

A degree of freedom is an intensive variable such as T, P, X_A, X_B, ... that can be varied independently while still maintaining equilibrium. If pressure is maintained constant one degree of freedom is lost and the phase rule becomes

$$P + F = C + 1 \tag{1.50}$$

At present we are considering binary alloys so that $C = 2$ therefore

$$P + F = 3$$

This means that a binary system containing one phase has two degrees of freedom, i.e., T and X_B can be varied independently. In a two-phase region of a phase diagram $P = 2$ and therefore $F = 1$, which means that if the temperature is chosen independently the compositions of the phases are fixed. When three phases are in equilibrium, such as at a eutectic or peritectic temperature, there are no degrees of freedom and the compositions of the phases and the temperature of the system are all fixed.

1.5.7 Effect of Temperature on Solid Solubility

The equations for free energy and chemical potential can be used to derive the effect of temperature on the limits of solid solubility in a terminal solid solution. Consider for simplicity the phase diagram shown in Figure 1.36a where B is soluble in A, but A is virtually insoluble in B. The corresponding free energy curves for temperature T_1 are shown schematically in Figure 1.36b. Since A is almost insoluble in B the G^β curve rises rapidly as shown. Therefore, the maximum concentration of B soluble in A(X_B^e) is given by the condition

$$\mu_B^\alpha = \mu_B^\beta \simeq G_B^\beta$$

For a regular solid solution Equation 1.40 gives

$$\mu_B^a = G_B^\alpha + \Omega(1 - X_B)^2 + RT \ln X_B$$

But from Figure 1.36b, $G_B^\alpha - \mu_B^\alpha = \Delta G_B$, the difference in free energy between pure B in the stable β-form and the unstable α-form. Therefore for $X_B = X_B^e$

$$-RT \ln X_B^e - \Omega(1 - X_B^e)^2 = \Delta G_B \tag{1.51}$$

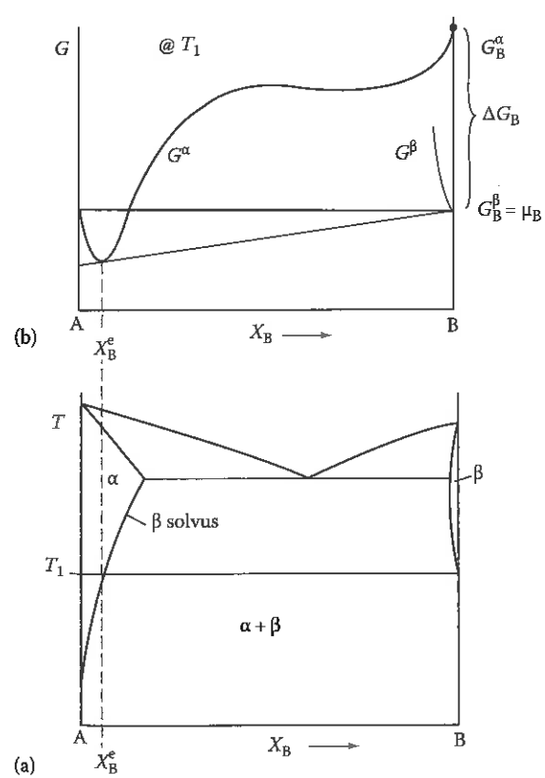

FIGURE 1.36
Solubility of B in A.

If the solubility is low $X_B^e \ll 1$ and this gives

$$X_B^e = \exp\left\{-\frac{\Delta G_B + \Omega}{RT}\right\} \tag{1.52}$$

Putting

$$\Delta G_B = \Delta H_B - T\Delta S_B$$

gives

$$X_B^e = A \exp\frac{-Q}{RT} \tag{1.53}$$

where A is a constant equal to $\exp(\Delta S_B/R)$ and

$$Q = \Delta H_B + \Omega \tag{1.54}$$

ΔH_B is the difference in enthalpy between the β-form of B and the α-form in J mol^{-1}. Ω is the change in energy when 1 mol of B with the α-structure dissolves in A to make a dilute solution. Therefore Q is just the enthalpy change, or heat absorbed, when 1 mol of B with the β-structure dissolves in A to make a dilute solution.

ΔS_B is the difference in entropy between β-B and α-B and is approximately independent of temperature. Therefore, the solubility of B in α increases exponentially with temperature at a rate determined by Q. It is interesting to note that, except at absolute zero, X_B^e can never be equal to zero, that is, no two components are ever completely insoluble in each other.

1.5.8 Equilibrium Vacancy Concentration

So far it has been assumed that in a metal lattice every atom site is occupied. However, let us now consider the possibility that some sites remain without atoms, that is, there are vacancies in the lattice. The removal of atoms from their sites not only increases the internal energy of the metal, due to the broken bonds around the vacancy, but also increases the randomness or configurational entropy of the system. The free energy of the alloy will depend on the concentration of vacancies, and the equilibrium concentration X_v^e will be that which gives the minimum free energy.

If, for simplicity, we consider vacancies in a pure metal the problem of calculating X_v^e is almost identical to the calculation of ΔG_{mix} for A and B atoms when ΔH_{mix} is positive. Because the equilibrium concentration of vacancies is small the problem is simplified because vacancy–vacancy interactions can be ignored and the increase in enthalpy of the solid (ΔH) is directly proportional to the number of vacancies added, i.e.,

$$\Delta H \simeq \Delta H_v X_v$$

where

X_v is the mole fraction of vacancies

ΔH_v is the increase in enthalpy per mole of vacancies added

Each vacancy causes an increase of $\Delta H_v/N_a$ where N_a is Avogadro's number.

There are two contributions to the entropy change ΔS on adding vacancies. There is a small change in the thermal entropy of ΔS_v per mole of vacancies added due to changes in the vibrational frequencies of the atoms around a vacancy. The largest contribution, however, is due to the increase in configurational entropy given by Equation 1.25. The total entropy change is thus

$$\Delta S = X_v \Delta S_v - R(X_v \ln X_v + (1 - X_v)\ln(1 - X_v))$$

The molar free energy of the crystal containing X_v mol of vacancies is therefore given by

$$G = G_A + \Delta G = G_A + \Delta H_v X_v - T\Delta S_v X_v + RT(X_v \ln X_v + (1 - X_v)\ln(1 - X_v)) \tag{1.55}$$

This is shown schematically in Figure 1.37. Given time the number of vacancies will adjust so as to reduce G to a minimum. The equilibrium concentration of vacancies X_v^e is therefore given by the condition

$$\left.\frac{dG}{dX_v}\right|_{X_v = X_v^e} = 0$$

Differentiating Equation 1.55 and making the approximation $X_v \ll 1$ gives

$$\Delta H_v - T\Delta S_v + RT \ln X_v^e = 0$$

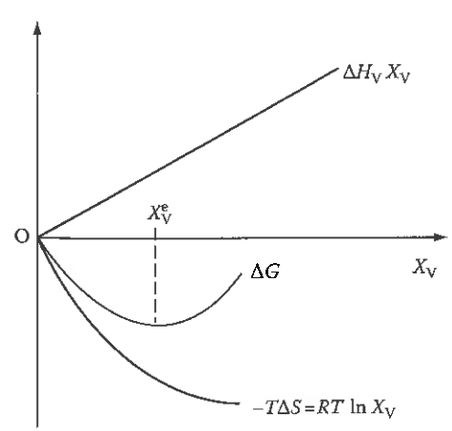

FIGURE 1.37
Equilibrium vacancy concentration.

Therefore, the expression for X_v^e is

$$X_v^e = \exp\frac{\Delta S_v}{R} \cdot \exp\frac{-\Delta H_v}{RT} \tag{1.56}$$

or, putting $\Delta G_v = \Delta H_v - T\Delta S_v$ gives

$$X_v^e = \exp\frac{-\Delta G_v}{RT} \tag{1.57}$$

The first term on the right-hand side of Equation 1.56 is a constant ~3, independent of T, whereas the second term increases rapidly with increasing T. In practice, ΔH_v is of the order of 1 eV per atom and X_v^e reaches a value of about 10^{-4} to 10^{-3} at the melting point of the solid.

1.6 Influence of Interfaces on Equilibrium

The free energy curves that have been drawn so far have been based on the molar free energies of infinitely large amounts of material of a perfect single crystal. Surfaces, grain boundaries, and interphase interfaces have been ignored. In real situations these and other crystal defects such as dislocations do exist and raise the free energies of the phases. Therefore the minimum free energy of an alloy, i.e., the equilibrium state, is not reached until virtually all interfaces and dislocations have been annealed out. In practice such a state is unattainable within reasonable periods of time.

Interphase interfaces can become extremely important in the early stages of phase transformations when one phase, β, say, can be present as very fine particles in the other phase, α, as shown in Figure 1.38a. If the α-phase is acted on by a pressure of 1 atm the β-phase is subjected to an extra pressure ΔP due to the curvature of the α/β interface, just as a soap bubble exerts an extra pressure ΔP on its contents. If γ is the α/β interfacial energy and the particles are spherical with a radius r, ΔP is given approximately by

$$\Delta P = \frac{2\gamma}{r}$$

By definition, the Gibbs free energy contains a PV term and an increase of pressure P therefore causes an increase in free energy G. From Equation 1.9 at constant temperature

$$\Delta G = \Delta P \cdot V$$

Therefore, the β curve on the molar free energy–composition diagram in Figure 1.38b will be raised by an amount

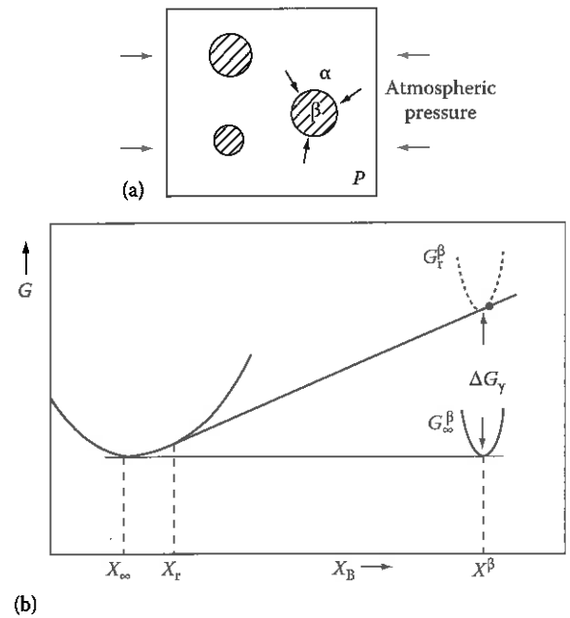

FIGURE 1.38
The effect of interfacial energy on the solubility of small particles.

$$\Delta G_\gamma = \frac{2\gamma V_m}{r} \tag{1.58}$$

where V_m is the molar volume of the β-phase. This free energy increase due to interfacial energy is known as a capillarity effect or the Gibbs–Thomson effect.

The concept of a pressure difference is very useful for spherical liquid particles, but it is less convenient in solids. This is because, as will be discussed in Chapter 3, finely dispersed solid phases are often nonspherical. For illustration, therefore, consider an alternative derivation of Equation 1.58 which can be more easily modified to deal with nonspherical cases.[3]

Consider a system containing two β particles, one with a spherical interface of radius r and the other with a planar interface ($r = \infty$) embedded in an α matrix as shown in Figure 1.39. If the molar free energy difference between the two particles is ΔG_γ, the transfer of a small quantity (dn mol) of β from the large to the small particle will increase the free energy of the system by a small amount (dG) given by

$$dG = \Delta G_\gamma dn$$

If the surface area of the large particle remains unchanged the increase in free energy will be due to the increase in the interfacial area of the spherical particle (dA). Therefore, assuming γ is constant

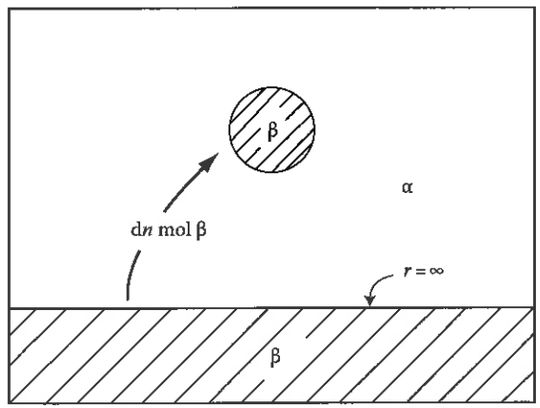

FIGURE 1.39
Transfer of dn mol of β from a large to a small particle.

$$dG = \gamma dA$$

Equating these two expressions gives

$$\Delta G_\gamma = \gamma \frac{dA}{dn} \tag{1.59}$$

Since $n = 4\pi r^3/3V_m$ and $A = 4\pi r^2$ it can easily be shown that

$$\frac{dA}{dn} = \frac{dA/dr}{dn/dr} = \frac{2V_m}{r}$$

from which Equation 1.58 can be obtained.

An important practical consequence of the Gibbs–Thomson effect is that the solubility of β in α is sensitive to the size of the β particles. From the common tangent construction in Figure 1.38b, it can be seen that the concentration of solute B in α in equilibrium with β across curved interface (X_r) is greater than X_∞, the equilibrium concentration for a planar interface. Assuming for simplicity that the α-phase is a regular solution and that the β-phase is almost pure B, i.e., $X_B^\beta \sim 1$, Equation 1.52 gives

$$X_\infty = \exp\left\{-\frac{\Delta G_B + \Omega}{RT}\right\}$$

Similarly X_r can be obtained by using $(\Delta G_B - 2\gamma V_m/r)$ in place of ΔG_B

$$X_r = \exp\left\{-\frac{\Delta G_B + \Omega - 2\gamma V_m/r}{RT}\right\}$$

Therefore,

$$X_r = X_\infty \exp\frac{2\gamma V_m}{RTr} \tag{1.60}$$

and for small values of the exponent

$$X_r \simeq X_\infty\left(1 + \frac{2\gamma V_m}{RTr}\right) \tag{1.61}$$

Taking the following typical values: $\gamma = 200$ mJ m^{-2}, $V_m = 10^{-5}$ m^3, $R = 8.31$ J mol^{-1} K^{-1}, $T = 500$ K gives

$$\frac{X_r}{X_\infty} \simeq 1 + \frac{1}{r\,(\text{nm})}$$

e.g., for $r = 10$ nm $X_r/X_\infty \sim 1.1$. It can be seen therefore that quite large solubility differences can arise for particles in the range $r = 1$–100 nm. However, for particles visible in the light microscope ($r > 1$ μm) capillarity effects are very small.

1.7 Ternary Equilibrium

Since most commercial alloys are based on at least three components, an understanding of ternary phase diagrams is of great practical importance. The ideas that have been developed for binary systems can be extended to systems with three or more components.[4]

The composition of a ternary alloy can be indicated on an equilateral triangle (the Gibbs triangle) whose corners represent 100% A, B, or C as shown in Figure 1.40. The triangle is usually divided by equidistant lines parallel to the sides marking 10% intervals in atomic or weight percent. All points on lines parallel to BC contain the same percentage of A, the lines parallel to AC represent constant B concentration, and lines parallel to AB constant C concentrations. Alloys on PQ for example contain 60% A, on RS 30% B, and TU 10% C. Clearly the total percentage must sum to 100%, or expressed as mole fractions

$$X_A + X_B + X_C = 1 \tag{1.62}$$

The Gibbs free energy of any phase can now be represented by a vertical distance from the point in the Gibbs triangle. If this is done for all possible compositions, the points trace out the free energy surfaces for all the possible phases, as shown in Figure 1.41a. The chemical potentials of A, B, and C in

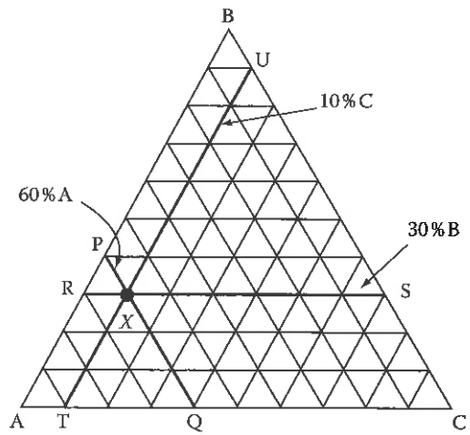

FIGURE 1.40
The Gibbs triangle.

any phase are then given by the points where the tangential plane to the free energy surfaces intersects the A, B, and C axes. Figure 1.41a is drawn for a system in which the three binary systems AB, BC, and CA are simple eutectics. Free energy surfaces exist for three solid phases α, β, and γ and the liquid phase, L. At this temperature the liquid phase is most stable for all alloy compositions. At lower temperatures the G^L surface moves upward and eventually intersects the G^α surface as shown in Figure 1.41b. Alloys with compositions in the vicinity of the intersection of the two curves consist of a + L at equilibrium. In order for the chemical potentials to be equal in both phases the compositions of the two phases in equilibrium must be given by points connected by a common tangential plane, for example, *s* and *l* in Figure 1.41b. These points can be marked on an isothermal section of the equilibrium phase diagram as shown in Figure 1.41c. The lines joining the compositions in equilibrium are known as tie-lines. By rolling the tangential plane over the two free energy surfaces a whole series of tie-lines will be generated, such as pr and qt, and the region covered by these tie-lines pqtr is a two-phase region on the phase diagram. An alloy with composition *x* in Figure 1.41c will therefore minimize its free energy by separating into solid α with composition *s* and liquid with composition *l*. The relative amounts of α and L are simply given by the lever rule. Alloys with compositions within Apq will be a homogeneous α-phase at this temperature, whereas alloys within BCrt will be liquid.

On further cooling the free energy surface for the liquid will rise through the other free energy surfaces producing the sequence of isothermal sections shown in Figure 1.42. In Figure 1.42f, for example, the liquid is stable near the center of the diagram whereas at the corners the α, β, and γ solid phases are stable. In between are several two-phase regions containing bundles of tie-lines. In addition there are three-phase regions known as tie-triangles. The L + α + β triangle for example arises because the common tangential plane simultaneously touches the G^α, G^β, and G^L surfaces. Therefore, any alloy

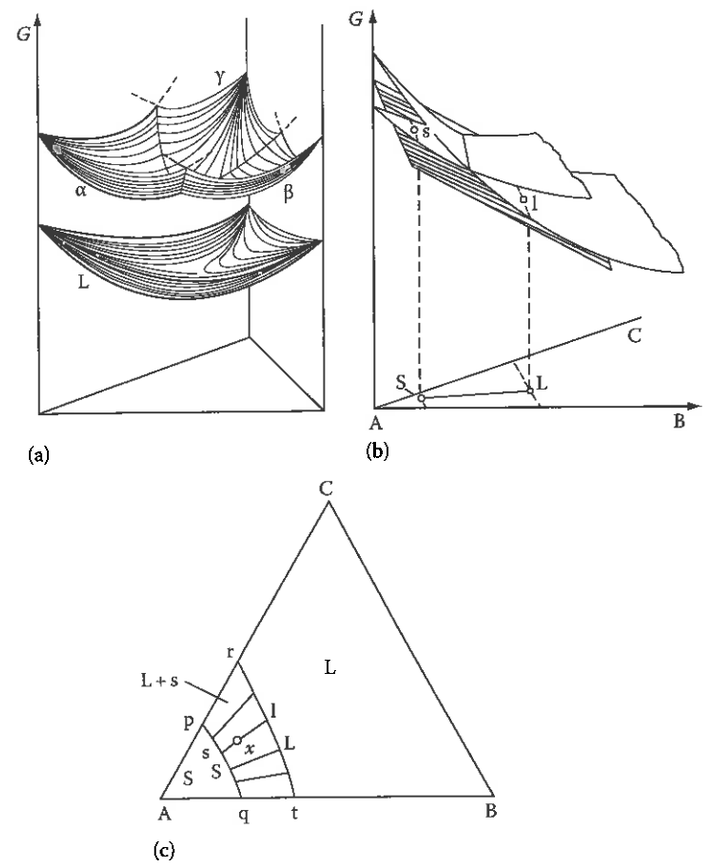

FIGURE 1.41
(a) Free energies of a liquid and three solid phases of a ternary system. (b) A tangential plane construction to the free energy surfaces defines equilibrium between *s* and *l* in the ternary system. (c) Isothermal section through a ternary phase diagram obtained in this way with a two-phase region (L + S) and various tie-lines. The amounts of *l* and *s* at point *x* are determined by the lever rule. (After Haasen, P., *Physical Metallurgy*, Cambridge University Press, Cambridge, 1978.)

with a composition within the L + α + β triangle at this temperature will be in equilibrium as a three-phase mixture with compositions given by the corners of the triangle. If the temperature is lowered still further the L region shrinks to a point at which four phases are in equilibrium L + α + β + γ. This is known as the ternary eutectic point and the temperature at which it occurs is the ternary eutectic temperature (Figure 1.42g). Below this temperature the liquid is no longer stable and an isothermal section contains three two-phase regions and one three-phase tie triangle α + β + γ as shown in Figure 1.42h. If isothermal sections are constructed for all temperatures they can be combined into a three-dimensional ternary phase diagram as shown in Figure 1.44.

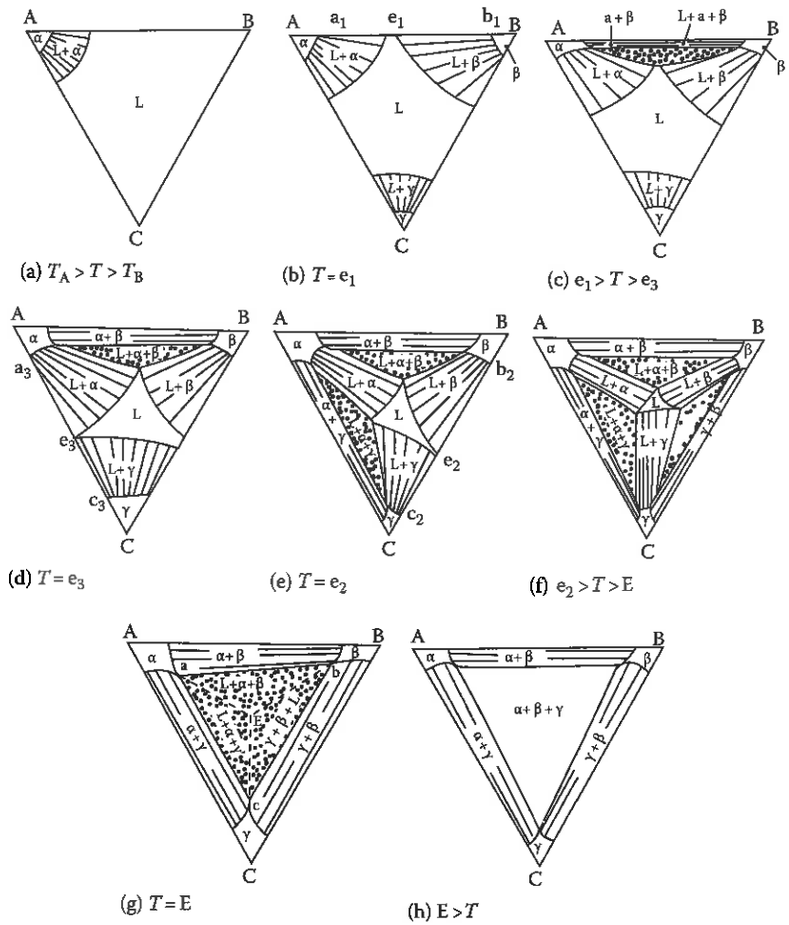

FIGURE 1.42
Isothermal sections through Figure 1.44. (After Prince, A., *Alloy Phase Equilibria*, Elsevier, Amsterdam, 1966.)

In order to follow the course of solidification of a ternary alloy, assuming equilibrium is maintained at all temperatures, it is useful to plot the liquidus surface contours as shown in Figure 1.43. During equilibrium freezing of alloy X the liquid composition moves approximately along the line Xe (drawn through A and X) as primary α-phase is solidified; then along the eutectic valley eE as both α and β solidify simultaneously. Finally at E, the ternary eutectic point, the liquid transforms simultaneously into $\alpha + \beta + \gamma$. This sequence of events is also illustrated in the perspective drawing in Figure 1.44.

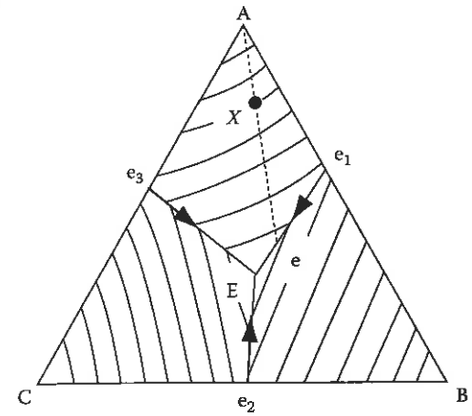

FIGURE 1.43
A projection of the liquidus surfaces of Figure 1.44 onto the Gibbs triangle.

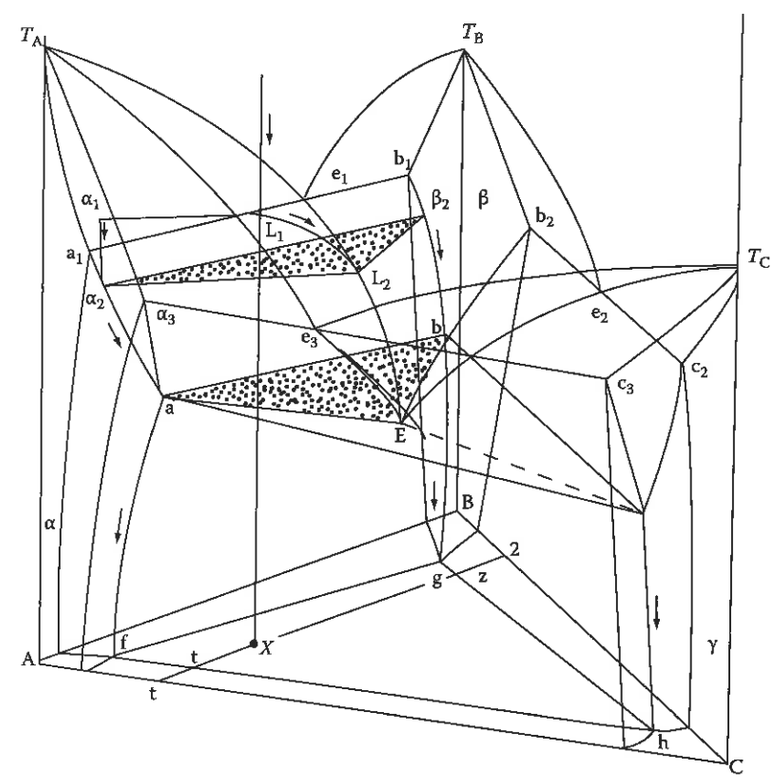

FIGURE 1.44
Equilibrium solidification of alloy X. (After Prince, A., *Alloy Phase Equilibria*, Elsevier, Amsterdam, 1966.)

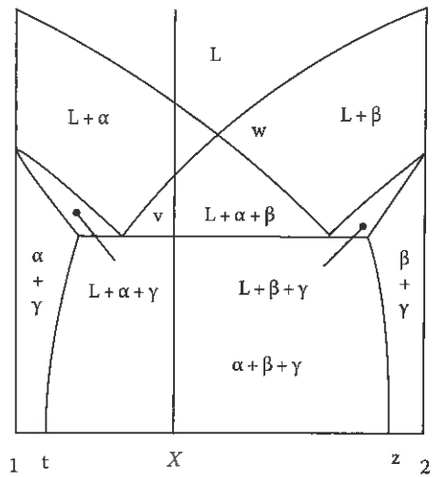

FIGURE 1.45
A vertical section between points 1, 2, and X in Figure 1.44. (After Prince, A., *Alloy Phase Equilibria*, Elsevier, Amsterdam, 1966.)

The phases that form during solidification can also be represented on a vertical section through the ternary phase diagram. Figure 1.45 shows such a section taken through X parallel to AB in Figure 1.44. It can be seen that on cooling from the liquid phase the alloy first passes into the $L+\alpha$ region, then into $L+\alpha+\beta$, and finally all liquid disappears and the $\alpha+\beta+\gamma$ region is entered, in agreement with the above.

An important limitation of vertical sections is that in general the section will not coincide with the tie-lines in the two-phase regions and so the diagram only shows the phases that exist in equilibrium at different temperatures and not their compositions. Therefore, they cannot be used like binary phase diagrams, despite the superficial resemblance.

1.8 Additional Thermodynamic Relationships for Binary Solutions

It is often of interest to be able to calculate the change in chemical potential ($d\mu$) that results from a change in alloy composition (dX). Considering Figure 1.46 and comparing triangles it can be seen that

$$-\frac{d\mu_A}{X_B} = \frac{d\mu_B}{X_A} = \frac{d(\mu_B - \mu_A)}{1} \tag{1.63}$$

and that the slope of the free energy–composition curve is given by

$$\frac{dG}{dX_B} = \frac{\mu_B - \mu_A}{1} \tag{1.64}$$

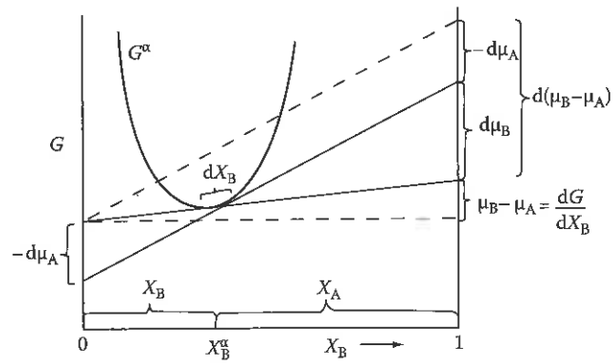

FIGURE 1.46
Evaluation of the change in chemical potential due to a change in composition. (After Hillert, M., in *Lectures on the Theory of Phase Transformations*, Aaronson, H.I. (Ed.), The American Society for Metals and The Metallurgical Society of AIME, New York, 1969.)

Substituting this expression into Equation 1.63 and multiplying throughout by $X_A X_B$ leads to the following equalities:

$$-X_A d\mu_A = X_B d\mu_B = X_A X_B \frac{d^2G}{dX^2} dX_B \tag{1.65}$$

which are the required equations relating $d\mu_A$, $d\mu_B$, and dX_B. The first equality in this equation is known as the Gibbs–Duhem relationship for a binary solution. Note that the subscript "B" has been dropped from d^2G/dX^2 as $d^2G/dX_B^2 = d^2G/dX_A^2$. For a regular solution differentiation of Equation 1.39 gives

$$\frac{d^2G}{dX^2} = \frac{RT}{X_A X_B} - 2\Omega \tag{1.66}$$

For an ideal solution $\Omega = 0$ and

$$\frac{d^2G}{dX^2} = \frac{RT}{X_A X_B} \tag{1.67}$$

Equation 1.65 can be written in a slightly different form by making use of activity coefficients. Combining Equations 1.41 and 1.43 gives

$$\mu_B = G_B + RT \ln \gamma_B X_B \tag{1.68}$$

Therefore,

$$\frac{d\mu_B}{dX_B} = \frac{RT}{X_B}\left\{1 + \frac{X_B}{\gamma_B}\frac{d\gamma_B}{dX_B}\right\} = \frac{RT}{X_B}\left\{1 + \frac{d\ln\gamma_B}{d\ln X_B}\right\} \tag{1.69}$$

A similar relationship can be derived for $d\mu_A/dX_B$. Equation 1.65 therefore becomes

$$-X_A d\mu_A = X_B d\mu_B = RT\left\{1+\frac{d\ln\gamma_A}{d\ln X_A}\right\}dX_B = RT\left\{1+\frac{d\ln\gamma_B}{d\ln X_B}\right\}dX_B \quad (1.70)$$

Comparing Equations 1.65 and 1.70 gives

$$X_A X_B \frac{d^2G}{dX^2} = RT\left\{1+\frac{d\ln\gamma_A}{d\ln X_A}\right\} = RT\left\{1+\frac{d\ln\gamma_B}{d\ln X_B}\right\} \quad (1.71)$$

1.9 Computation of Phase Diagrams

The determination of Gibbs energy of phases, with various properties, pure stoichiometric substances for instance, as a function of temperature, composition, and pressure is necessary for establishing a thermodynamic databank. As described earlier, if Gibbs energy is known, other thermodynamic properties like enthalpy and entropy could easily be derived. Thermodynamic information gathered by conducting experiments are usually compared against existing physical models the purpose of which is to quantify and give predictions of the measured thermodynamic properties. However, it is important to realize that such models could yield unreliable predictions if used outside the range over which they were verified.

1.9.1 Pure Stoichiometric Substances

Thermodynamic data of pure stoichiometric substances are stored as the enthalpy of formation and entropy measured at room temperature (298.15 K) and 1 bar atmospheric pressure (called henceforth the standard conditions), in addition to heat capacity[5]

$$H = H^{\text{ref}} + \int_{T_{\text{ref}}}^{T} C_p dT \quad (1.72)$$

$$S = S^{\text{ref}} + \int_{T_{\text{ref}}}^{T} \frac{C_p}{T} dT \quad (1.73)$$

where the new values of H and S can be determined as a function of temperature compared with a reference state. Note that the second term in the enthalpy and entropy equations is essentially the same as shown in Equations 1.6 and 1.8, respectively.

Gibbs energy could then be estimated from Gibbs–Helmholtz relationship $G = H - TS$. Therefore, obviously it is necessary to describe the heat capacity as a function of temperature.

The Debye function expresses the heat capacity as a function of temperature as follows:

$$C = D\left(\frac{\Theta}{T}\right) \quad (1.74)$$

where Θ is the Debye temperature which can be written as

$$\Theta = \frac{h\omega_D}{2\pi k} \quad (1.75)$$

where

h and k are the Planck and Boltzmann constants, respectively
ω_D is defined as the Debye frequency

The Debye temperature is a material-dependent constant. As atoms vibrate, such vibration increases with temperature yet not all atoms vibrate with the same frequency. When deriving the internal energy due to lattice vibrations, a spectrum is considered, the maximum frequency of which is called the Debye frequency. However, such an approach may not be suitable for determining all the experimental thermodynamic values of solid substances.[6]

According to Hack,[5] a system of thermochemical data was introduced based on the so-called standard element reference state (SER). That is to say, the enthalpy of a state of elements stable under the standard conditions is set to zero, by convention, at these conditions. The entropy, however, takes the absolute value under these conditions.

After Mayer and Kelley,[7] a polynomial is then used to represent the relation between specific heat capacity at constant pressure, C_p, and temperature as follows:

$$C_p = C_1 + C_2T + C_3T^2 + \frac{C_4}{T^2} \quad (1.76)$$

The above relation can be used to describe most experimental data adequately by adjusting its empirical fitting parameters. However, as shown in Figure 1.47, the use of more than one function is sometimes necessary.

Consequently, under standard conditions, the Gibbs energy can be written as follows:

$$G = C_1 + C_2T + C_3T\ln(T) + C_4T^2 + C_5T^3 + \frac{C_6}{T} \quad (1.77)$$

These fitting parameters, C_i, are then stored in the Gibbs energy databank.

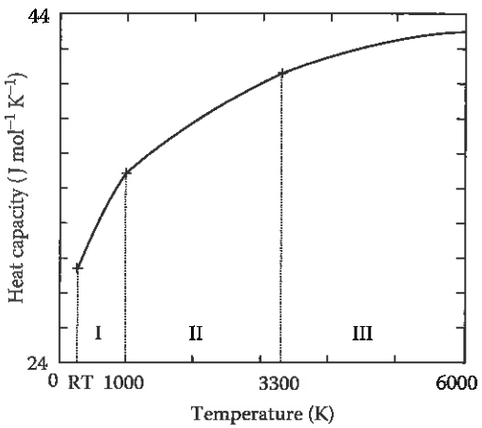

FIGURE 1.47
Heat capacity of oxygen gas versus temperature.[5] Note the use of several polynomials over different temperature ranges to best fit the measured data. (After Hack, K., in *The SGTE Casebook: Thermodynamics at Work*, Hack, K. (Ed.), The Institute of Materials, London, 1996.)

Contributions to Gibbs energy of pure stoichiometric phases such as metallic elements or stoichiometric oxides, SiO_2 for example, include those arising from the lattice, magnetic as well as pressure contributions

$$G_m = G_{lattice} + G_{magnetic} + G_{pressure} \tag{1.78}$$

where $G_{lattice}$ is a function of ΔH and S under the standard conditions, as well as the polynomial representing C_p. Other contributions to the Gibbs energy are discussed in the following section.

When applying the above scheme to substances exhibiting second-order magnetic phase transitions, where the shape of the heat capacity curve shows a rather sudden change, many polynomials are used around Curie temperature.[8] However, this approach has numerical limitations given the large number of fitting parameters needed, and also their large values. Inden suggested that exceptional changes in C_p should be treated separately.[9,10]

For the case of a magnetic phase transition, the magnetic contribution to Gibbs energy can be written as

$$G_{magnetic} = RTf\left(\frac{T}{T_c}\right)\ln(\beta + 1) \tag{1.79}$$

where

f is a structure-dependent function of temperature
T_c is a critical temperature which could be either Curie or Néel temperature
β is the magnetic moment per atom in the lattice

Note that f will differ in the temperature ranges below and above the critical temperature.

For a complete description of the Gibbs free energy, it is also necessary to consider the contribution caused by the effect of pressure on the molar volume. The SGTE consortium[5] followed the approach suggested by Murnaghan[11]

$$G_{pressure} = V^0 \exp\left[\int_{298}^{T} \alpha(T)dT\right] \frac{[1 + nK(T)P]^{(1-(1/n))} - 1}{(n-1)K(T)} \tag{1.80}$$

where

V^0 is the molar volume at room temperature
$\alpha(T)$ is the thermal expansion of that volume
n is the pressure derivative of the bulk modulus which is the inverse of the compressibility

$K(T)$ is a polynomial function of temperature which stands for the compressibility at a pressure of 1 bar

$$K(T) = K_0 + K_1T + K_2T^2 \tag{1.81}$$

The thermal expansion function, $\alpha(T)$, may be written as

$$\alpha(T) = A_0 + A_1T + A_2T^2 + \frac{A_3}{T^2} \tag{1.82}$$

An example of a calculated pressure–temperature phase diagram is shown in Figure 1.48.

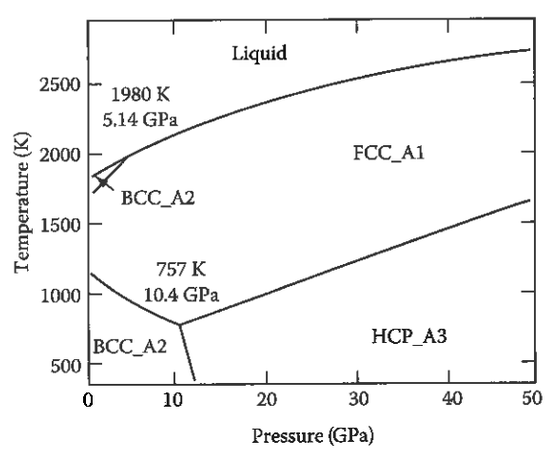

FIGURE 1.48
Pressure–temperature phase diagram of iron, calculated. (After Hack, K., in *The SGTE Casebook: Thermodynamics at Work*, Hack, K. (Ed.), The Institute of Materials, London, 1996.)

1.9.2 Solution Phases

1.9.2.1 Substitutional Solutions

In Section 1.3.2, we discussed ideal solutions where the free energy of such solutions was presented in Equation 1.27. For a multicomponent ideal solution, Equation 1.27 may be written as follows:

$$G^{id} = RT\sum X_i \ln(X_i) + \sum X_i G_i \tag{1.83}$$

where X_i is the mole fraction of constituent i. However, there is a need for mathematical expressions describing the deviation from the ideal solution, i.e., the excess Gibbs energy. These expressions should allow the estimation of thermodynamic properties of higher order systems from those measured on lower order systems.

Redlich and Kister[12] suggested determining the properties of a ternary system, say A–B–C, from the three binaries (A–B, A–C, and B–C). Therefore, for a binary solution with constituents A and B, say, the excess Gibbs energy may be described as

$$G^{ex}_{AB} = X_A X_B \sum L^{(i)}_{AB}(X_A - X_B)^i \tag{1.84}$$

So by fitting experimental data of a binary A–B to this relation, the parameters can be determined. When $i=0$, the excess energy is $X_A X_B L^{(0)}_{AB}$, a term which is that of the regular solution model, see Equation 1.36. Here the parameter $L^{(0)}_{AB}$ is independent from chemical composition. Other $L^{(i)}_{AB}$ parameters, when $i>0$, describe the composition dependence of parameter L_{AB}. Parameter L_{AB} is an energy parameter which is called the interaction energy. So the excess Gibbs energy for a ternary solution A–B–C may be written as a first approximation:

$$\begin{aligned} G^{ex}_{ABC} = {} & X_A X_B \sum L^{(i)}_{AB}(X_A - X_B)^i + X_A X_C \sum L^{(i)}_{AC}(X_A - X_C)^i \\ & + X_B X_C \sum L^{(i)}_{BC}(X_B - X_C)^i \end{aligned} \tag{1.85}$$

Logically, when experimental data are available for ternary solutions the measured properties should be compared against those predicted by Redlich–Kister approach. Any possible deviation should first be dealt with by adding a term $X_A X_B X_C L^{(0)}_{ABC}$ to the excess Gibbs energy. If the deviation is not adequately corrected for, the term could be formulated as

$$\begin{aligned} & X_A X_B X_C \left[L^{(0)}_{ABC} + \frac{1}{3}(1 + 2X_A - X_B - X_C) L^{(1)}_{ABC} + \frac{1}{3}(1 + 2X_B - X_C - X_A) L^{(1)}_{BCA} \right. \\ & \left. + \frac{1}{3}(1 + 2X_C - X_A - X_B) L^{(1)}_{CAB} \right] \end{aligned} \tag{1.86}$$

For quaternary systems, often there is no information regarding all four ternary systems and sometimes the data of the quaternary system itself are not available. Nevertheless, a quaternary term $X_A X_B X_C X_D L^{(0)}_{ABCD}$ may be added to the excess Gibbs energy in this case.

For other phases with different properties such as interstitial solutions, the reader is referred to, for example, Hack,[5] for further information.

1.10 Kinetics of Phase Transformations

The thermodynamic functions that have been described in this chapter apply to systems that are in stable or metastable equilibrium. Thermodynamics can therefore be used to calculate the driving force for a transformation (Equation 1.4), but it cannot say how fast a transformation will proceed. The study of how fast processes occur belongs to the science of kinetics.

Let us redraw Figure 1.1 for the free energy of a single atom as it takes part in a phase transformation from an initially metastable state into a state of lower free energy (Figure 1.49). If G_1 and G_2 are the free energies of the initial and final states, the driving force for the transformation will be $\Delta G = G_2 - G_1$. However, before the free energy of the atom can decrease from G_1 to G_2 the atom must pass through a so-called transition or activated state with a free energy ΔG^a above G_1. The energies shown in Figure 1.49 are average energies associated with large numbers of atoms. As a result of the random thermal motion of the atoms the energy of any particular atom will vary with time and occasionally it may be sufficient for the atom to reach the activated state. This process is known as thermal activation.

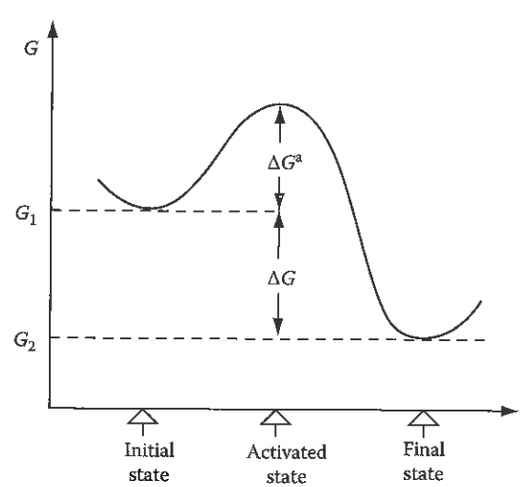

FIGURE 1.49
Transformation from initial to final state through an activated state of higher free energy.

According to kinetic theory, the probability of an atom reaching the activated state is given by $\exp(-\Delta G^a/kT)$ where k is Boltzmann's constant (R/N_a) and ΔG^a is known as the activation free energy barrier. The rate at which a transformation occurs will depend on the frequency with which atoms reach the activated state. Therefore, we can write

$$\text{Rate} \propto \exp\left(-\frac{\Delta G^a}{kT}\right)$$

Putting $\Delta G^a = \Delta H^a - T\Delta S^a$ and changing from atomic to molar quantities enables this equation to be written as

$$\text{Rate} \propto \exp\left(\frac{\Delta H^a}{RT}\right) \tag{1.87}$$

This equation was first derived empirically from the observed temperature dependence of the rate of chemical reactions and is known as the Arrhenius rate equation. It is also found to apply to a wide range of processes and transformations in metals and alloys, the simplest of these is the process of diffusion which is discussed in Chapter 2.

Exercises

1.1 The specific heat of solid copper above 300 K is given by

$$C_p = 22.64 + 6.28 \times 10^{-3} T \text{ J mol}^{-1}\text{K}^{-1}$$

By how much does the entropy of copper increase on heating from 300 to 1358 K?

1.2 With the aid of Equation 1.11 and Figure 1.5, draw schematic free energy–pressure curves for pure Fe at 1600°C, 800°C, 500°C, and 300°C.

1.3 Estimate the change in the equilibrium melting point of copper caused by a change of pressure of 10 kbar. The molar volume of copper is 8.0×10^{-6} m^3 for the liquid, and 7.6×10^{-6} m^3 for the solid phase. The latent heat of fusion of copper is 13.05 kJ mol^{-1}. The melting point is 1085°C.

1.4 For a single-component system, why do the allotropes stable at high temperatures have higher enthalpies than allotropes stable at low temperatures, e.g., $H(\gamma\text{-Fe}) > H(\alpha\text{-Fe})$?

1.5 Determine, by drawing, the number of distinguishable ways of arranging two black balls and two white balls in a square array. Check your answer with Equation 1.24.

1.6 By using Equations 1.30 and 1.31, show that the chemical potentials of A and B can be obtained by extrapolating the tangent to the G–X curve to $X_A = 0$ and $X_B = 0$.

1.7 Derive Equation 1.40 from Equations 1.31 and 1.39.

1.8 15 g gold and 25 g of silver are mixed to form a single-phase ideal solid solution.
- a. How many moles of solution are there?
- b. What are the mole fractions of gold and silver?
- c. What is the molar entropy of mixing?
- d. What is the total entropy of mixing?
- e. What is the molar free energy change at 500°C?
- f. What are the chemical potentials of Au and Ag at 500°C taking the free Au atom is added? Express your answer in eV atom^{-1}.
- g. By how much will the free energy of the solution change at 500°C if one Au atom is added? Express your answer in eV atom^{-1}.

1.9 In the Fe–C system Fe_3C is only a metastable phase, while graphite is the most stable carbon-rich phase. By drawing schematic free energy–composition diagrams show how the Fe-graphite phase diagram compares to the Fe–Fe_3C phase diagram from 0 to 2 wt% Fe. Check your answer with the published phase diagram in the *Metals Handbook* for example.

1.10 Consider a multicomponent system A, B, C,... containing several phases α, β, γ,... at equilibrium. If a small quantity of A (dn_A mol) is taken from the α-phase and added to the β-phase at constant T and P what are the changes in the free energies of the α- and β-phases, dG^α and dG^β? Since the overall mass and composition of the system is unchanged by the above process the total free energy change $dG = dG^\alpha + dG^\beta = 0$. Show, therefore, that $\mu_A^\alpha = \mu_A^\beta$. Repeating for other pairs of phases and other components gives the general equilibrium conditions, Equation 1.48.

1.11 For aluminum $\Delta H_v = 0.8$ eV atom^{-1} and $\Delta S_v/R = 2$. Calculate the equilibrium vacancy concentration at 660°C (T_m) and 25°C.

1.12 The solid solubility of silicon in aluminum is 1.25 atomic % at 550°C and 0.46 atomic % at 450°C. What solubility would you expect at 200°C? Check your answer by reference to the published phase diagram.

1.13 The metal A and metal B form an ideal liquid solution but are almost immiscible in the solid state. The entropy of fusion of both A and B is 8.4 J mol^{-1} K^{-1} and the melting temperatures are 1500 and 1300 K, respectively. Assuming that the specific heats of the solid and liquid are identical calculate the eutectic composition and temperature in the A–B phase diagram.

1.14 Write down an equation that shows by how much the molar free energy of solid Cu is increased when it is present as a small sphere of radius r in liquid Cu. By how much must liquid Cu be cooled below T_m before a solid particle of Cu can grow if the particle diameter is (1) 2 μm, (2) 2 nm (20 Å)? (Cu: $T_m = 1085°C = 1358$ K. Atomic weight 63.5.

Density 8900 kg m^{-3}. Solid/liquid interfacial energy $\gamma = 0.144$ J m^{-2}. Latent heat of melting $L = 13{,}300$ J mol^{-1}.)

1.15 Suppose a ternary alloy containing 40 atomic % A, 20 atomic % B, 40 atomic % C solidifies through a ternary eutectic reaction to a mixture of α, β, and γ with the following compositions: 80 atomic % A, 5 atomic % B, 15 atomic % C; 70 atomic % B, 10 atomic % A, 20 atomic % C; and 20 atomic % B, 10 atomic % A, 70 atomic % C. What will be the mole fractions of α, β, and γ in the microstructure?

1.16 Show that a general expression for the chemical potential of a component in solution is given by

$$\mu_A = G_A^0 + S_A(T_0 - T) + RT \ln \gamma_A X_A + (P - P_0)V_m$$

where

G_A^0 is the free energy of pure A at temperature T_0 and pressure P_0
S_A is the entropy of A
R is the gas constant
γ_A is the activity coefficient for A
X_A is the mole fraction in solution
V_m is the molar volume which is assumed to be constant

Under what conditions is the above equation valid?

References

1. D.R. Gaskell, *Introduction to Metallurgical Thermodynamics*, McGraw-Hill, New York, 1973, p. 342.
2. R.W. Cahn (Ed.), *Physical Metallurgy*, 2nd edn., Chapters 4 and 5, North-Holland, Amsterdam, 1974.
3. M. Ferrante and R.D. Doherty, *Acta Metall.*, 27: 1603, 1979.
4. M. Hillert, *Phase Transformations*, Chapter 5, American Society for Metals, Metals Park, OH, 1970.
5. K. Hack (Ed.), *The SGTE Casebook: Thermodynamics at Work*, Part 1, Institute of Materials, London, 1996.
6. C. Gerthsen and H.O. Kneser, *Physik*, Springer Verlag, Berlin, Heidelberg, New York, 1969.
7. K.K. Kelley, *US Bureau of Mines Bulletin 476*, 1949.
8. I. Barin and O. Knache, Springer-Verlag, Berlin, Heidelberg, and Verlag Stahleisen, Düsseldorf, 1973.
9. G. Inden, *Proc. of Calphad V*, Düsseldorf, III.4, 1–13, 1976.
10. G. Inden, *Proc. of Calphad V*, Düsseldorf, IV.1, 1–33, 1976.
11. F.D. Murnaghan, *Proc. Natl. Acad. Sci. (USA)*, 30: 244, 1944.
12. O. Redlich and A.T. Kister, *Ind. Eng. Chem.*, 40: 345–348, 1948.

Further Reading

A.H. Cottrell, Alloys (Chapter 14), The phase diagram (Chapter 15), in *An Introduction to Metallurgy*, Edward Arnold, London, 1967.

D.R. Gaskell, *Introduction to Metallurgical Thermodynamics*, McGraw-Hill, New York, 1973.

P. Gordon, *Principles of Phase Diagrams in Materials Systems*, McGraw-Hill, New York, 1968.

M. Hillert, Calculation of phase equilibria, in *Phase Transformations*, Chapter 5, American Society for Metals, Metals Park, OH, 1970.

M. Hillert, The uses of the Gibbs free energy–composition diagrams, in H.I. Aaronson (Ed.), *Lectures on the Theory of Phase Transformations*, Chapter 1, The Metallurgical Society of AIME, New York, 1975.

C.H.P. Lupis, *Chemical Thermodynamics of Materials*, North Holland, Amsterdam, 1983.

A.D. Pelton, Phase diagrams, in R.W. Cahn and P. Haasen (Eds.), *Physical Metallurgy*, Chapter 7, North-Holland, Amsterdam, 1983.

A. Prince, *Alloy Phase Equilibria*, Elsevier, London, 1966.

G.V. Raynor, Phase diagrams and their determination, in R.W. Cahn (Ed.), *Physical Metallurgy*, Chapter 7, North-Holland, Amsterdam, 1970.

F.N. Rhines, *Phase Diagrams in Metallurgy*, McGraw-Hill, New York, 1956.

P.G. Shewmon, Metallurgical thermodynamics, in R.W. Cahn and P. Haasen (Eds.), *Physical Metallurgy*, Chapter 6, North-Holland, Amsterdam, 1983.

R.A. Swalin, *Thermodynamics of Solids*, 2nd edn., Wiley, New York, 1972.

D.R.F. West, *Ternary Equilibrium Diagrams*, 2nd edn., Chapman & Hall, London, U.K., 1982.